Unified preserving properties of kinetic schemes

Zhaoli Guo [1,*] Jiequan Li [2,†] and Kun Xu [3,‡]

[1]*Institute of Multidisciplinary Research for Mathematics and Applied Science, Huazhong University of Science and Technology, Wuhan 430074, China*

[2]*Academy of Multidisciplinary Studies, Capital Normal University, Beijing 100048, China*

[3]*Department of Mathematics, Hong Kong University of Science and Technology, Clear Water Bay, Hong Kong, China*

(Received 25 October 2022; accepted 19 January 2023; published 6 February 2023)

The kinetic theory provides a physical basis for developing multiscale methods for gas flows covering a wide range of flow regimes. A particular challenge for kinetic schemes is whether they can capture the correct hydrodynamic behaviors of the system in the continuum regime (i.e., as the Knudsen number $\epsilon \ll 1$) without enforcing kinetic scale resolution. At the current stage, the main approach to analyze such a property is the asymptotic preserving (AP) concept, which aims to show whether a kinetic scheme reduces to a solver for the hydrodynamic equations as $\epsilon \to 0$, such as the shock capturing scheme for the Euler equations. However, the detailed asymptotic properties of the kinetic scheme are indistinguishable when ϵ is small but finite under the AP framework. To distinguish different characteristics of kinetic schemes, in this paper we introduce the concept of unified preserving (UP) aiming at assessing asymptotic orders of a kinetic scheme by employing the modified equation approach and Chapman-Enskon analysis. It is shown that the UP properties of a kinetic scheme generally depend on the spatial and temporal accuracy and closely on the interconnections among three scales (kinetic scale, numerical scale, and hydrodynamic scale) and their corresponding coupled dynamics. Specifically, the numerical resolution and specific discretization of particle transport and collision determine the flow physics of the scheme in different regimes, especially in the near continuum limit. As two examples, the UP methodology is applied to analyze the discrete unified gas-kinetic scheme and a second-order implicit-explicit Runge-Kutta scheme in their asymptotic behaviors in the continuum limit.

DOI: 10.1103/PhysRevE.107.025301

I. INTRODUCTION

In recent years there are increasing interests on simulating multiscale gas flows in different flow regimes covering a wide range of Knudsen numbers, defined as $\epsilon = \hat{\lambda}_0/\hat{l}_0 \sim \hat{\tau}_0/\hat{t}_0$, where $\hat{\lambda}_0$ and $\hat{\tau}_0$ are the typical mean free path and collision time of gas molecules, $\hat{l}_0$ and $\hat{t}_0$ are the characteristic hydrodynamic length and time scales, respectively. It is a challenging problem for modeling and simulating such flows due to the large spans of temporal and/or spatial scales under a wide range of physical scenarios, and it becomes even more complicated at discrete levels with involvement of mesh size and time step scales [1]. The classical computational fluid dynamics methods based on the Euler or Navier-Stokes equations are limited to continuum flows, while the kinetic particle methods, such as the direct simulation Monte Carlo, are mainly suitable for rarefied flows and encounter difficulties for continuum and near continuum flows.

However, it is well understood that gas kinetic models (Boltzmann or model equations) defined on the kinetic scale can lead to the Euler and Navier-Stokes equations on the hydrodynamic scale, and the gas kinetic theory provides a solid basis for developing schemes uniformly for flows from kinetic to hydrodynamic regimes. Therefore, developing deterministic numerical methods based on gas kinetic theory, which we call *kinetic schemes*, has attracted much attention. Actually, a variety of such schemes have been developed from different point of views in recent years, such as the lattice Boltzmann equation (LBE) method [2], gas-kinetic scheme (GKS) [3], semi-Lagrangian method [4], implicit-explicit (IMEX) method [5], unified gas-kinetic scheme (UGKS) [6], and discrete unified gas-kinetic scheme (DUGKS) [7]. It is noted that the LBE and GKS are kinetic solvers for the Navier-Stokes equations, while the UGKS and DUGKS are designed mainly for multiscale flows. The progress of numerical methods based on the kinetic equations can be found in a recent review article [8] and references therein.

The asymptotic behavior of the Boltzmann equation at small ϵ can be assessed by asymptotic analysis under certain scaling of the flow, such as the Chapman-Enskog analysis under acoustic scaling. Generally, the Chapman-Enskog solution of the nondimensional Boltzmann equation can be expressed as $f(\epsilon; \boldsymbol{x}, t) = \sum_{k=0}^{\infty} \epsilon^k f^{(k)}(\boldsymbol{x}, t)$, where the coefficients $f^{(k)}$ can be determined iteratively at the consecutive order of ϵ. Here $\boldsymbol{x} = \hat{\boldsymbol{x}}/\hat{l}_0$ and $t = \hat{t}/\hat{t}_0$ are the dimensionless space and time variables, respectively, while the hatted variables are the corresponding dimensional ones. Although the Chapman-Enskog approximation may deviate from the true solution, it can provide some useful asymptotics information at small

*zlguo@mail.hust.edu.cn
†jiequan@cnu.edu.cn
‡makxu@ust.hk

ϵ. For instance, the solution is consistent with the Euler and Navier-Stokes equations at the zeroth and first orders of ϵ, respectively.

For a kinetic scheme, in addition to the kinetic and hydrodynamic scales, numerical time and length scales (time step $\Delta\hat{t}$ and mesh size $\Delta\hat{\boldsymbol{x}}$) are also involved, and its asymptotic behaviors will become more complicated. Furthermore, its capability of capturing accurate solutions in the transition regime between kinetic and hydrodynamic ones depends closely on its limiting solution in the continuum regime with the hydrodynamic scale resolution. Therefore, it is critical to make a reliable assessment of the asymptotic behaviors of a kinetic scheme. Generally, a numerical solution f_h of the (nondimensional) Boltzmann equation depends on the mesh size $\Delta x = \Delta\hat{\boldsymbol{x}}/\hat{l}_0$ and time step $\Delta t = \Delta\hat{t}/\hat{t}_0$ in addition to ϵ, i.e., $f_h = f_h(\epsilon; \Delta x, \Delta t; \boldsymbol{x}, t)$. Here h indexes the discrete scale $h = (\Delta x, \Delta t)$. If the numerical scheme is a good discretization of the Boltzmann equation, then it can be expected that $f_h(\epsilon; \Delta x, \Delta t) \to f(\epsilon)$ as $\Delta x \to 0$ and $\Delta t \to 0$ for a fixed ϵ, such that f_h, like f, is consistent with the hydrodynamic equations for small ϵ. However, the computational burden may be extremely intensive if the scheme requires $\Delta x \ll \epsilon$ and/or $\Delta t \ll \epsilon$ for a valid hydrodynamic solution, such as Navier-Stokes ones. A practical kinetic scheme should be able to give a solution without resolving the kinetic scales, from which reliable numerical solutions of the hydrodynamic equations can be obtained, such as those direct Navier-Stokes solvers from discretizing the Navier-Stokes equations without imposing the mesh size and time step scales on the particle mean free path and collision time scales. Therefore, the current question is whether, and how much, f_h can be consistent with the corresponding hydrodynamic equations as $\Delta x \gg \epsilon$ and $\Delta t \gg \epsilon$ (i.e., $\Delta\hat{\boldsymbol{x}} \gg \hat{\lambda}_0$ and $\Delta\hat{t} \gg \hat{\tau}_0$).

Currently, the most popular approach to analyze the asymptotic behaviors of a kinetic scheme is to check its asymptotic preserving (AP) property, which is about to identify a consistent and stable discretization of the hydrodynamic equations in the limit of $\epsilon \to 0$ without resolving the kinetic scales [9,10].

Historically, the study of AP properties of numerical schemes for kinetic equations can be traced back to the pioneering work of Larsen [11], where the asymptotic behaviors of several spatial differencing schemes for the steady neutron transport equation were analyzed in the diffusion limit ($\epsilon_n \to 0$) with a fixed spatial mesh Δx, via an asymptotic expansion of the numerical scheme with respect to the neutron Knudsen number ϵ_n. The methodology was systematized later by considering the diffusive asymptotic behavior of numerical schemes under different mesh scales [12]. The approach was also employed to analyze and design numerical schemes for time-dependent transport equation with the diffusive scaling [13] and hyperbolic systems with stiff relaxation terms [14]. Particularly, a concrete definition of AP scheme was presented in the analysis of numerical methods for a linear hyperbolic system containing a stiff relaxation [15], focusing on the spatial discretizations.

The AP concept was also employed to analyze and develop kinetic schemes for flow problems. For instance, early in 1991, a time-splitting scheme for the Bhatnagar-Gross-Krook (BGK) equation was already proposed such that it can preserve the Euler limit [16] under acoustic scaling, and a finite-difference scheme for the Boltzmann equation, which can capture the incompressible Navier-Stokes equations under diffusive scaling, was developed later [17]. Actually, a large number of kinetic schemes with AP properties have been devised in the past three decades, such as the IMEX method [5], micro-macro decomposition method [18], and penalty method [19]. Several review papers at different periods summarized the progress on this subject [8,10,20].

The literature review reveals several important points about the state of art of the AP methodology:

(i) Most studies focus on the leading order asymptotics ($\epsilon \to 0$) of kinetic methods under different scalings, such as the Euler limit under the acoustic scaling (e.g., Refs. [16,21]) or incompressible Navier-Stokes limit under the diffusive scaling (e.g., Refs. [17,22]). Only a few schemes have been developed with the consideration of nonleading order (i.e., compressible Navier-Stokes) asymptotics for $0 < \epsilon \ll 1$ under the acoustic scaling [5,18,19,23,24]. However, it should be noted that it is implausible to use the AP framework for the analysis of nonleading order asymptotic behaviors since the AP concept is defined by the limiting behavior as the scaling parameter approaches to zero [9].

(ii) In most previous studies, the time asymptotics and space asymptotics are usually considered independently even though a few fully discrete kinetic schemes were analyzed, e.g., Refs. [18,24]. Indeed, when attention is paid on the time asymptotics, the spatial gradient is assumed to be discretized exactly or the influence of spatial discretization is ignored (e.g., Refs. [5,19,21–23,25,26]). In contrast, when spatial asymptotics is concerned, the semidiscrete form of kinetic equations is taken. In other words, the time integration is assumed to be precise. For example, several semidiscrete schemes for nonstationary hyperbolic systems were analyzed [15,27], where it was shown that the flux reconstruction is critical for space asmyptotics, as already demonstrated in Ref. [12] for the steady neutron transport equation. For time-dependent problems, the time evolution and spatial gradients interact mutually. In practical applications, the temporal-spatial coupling feature becomes important to capture correct physics [28]. Consequently, the temporal-spatial decoupled discretizations may lead to large numerical dissipations and thus influence the asymptotics, as argued and numerically verified in Ref. [29] by simulating the steady cavity flow. It is noted that some kinetic schemes with temporal-spatial coupling have been developed in recent years, such as the UGKS [6] and DUGKS [7] methods. In both methods, the flux at cell interface is reconstructed based on evolution solutions of the kinetic equation itself, and thus the coupled particle transport and collision in the temporal-spatial evolution is fully incorporated into the numerics. Indeed, a number of previous studies have demonstrated the distinguished features of these methods [6,29,30]. We will further demonstrate the importance of coupled transport and collision in designing kinetic schemes in the present work.

(iii) The standard procedure of asymptotic analysis in the AP framework is to verify whether a numerical scheme for the kinetic equation reduces to a consistent and stable scheme of the hydrodynamic (Euler or Navier-Stokes) equations, where Δx and Δt are fixed and independent of the

scaling parameter ϵ [8,10]. Many kinetic schemes with either Euler or (in)compressible Navier-Stokes asymptotics have been analyzed following this procedure, e.g., Refs. [17,18,24]. An alternative but more insightful approach for asymptotic analysis is to make use of the modified equation of the kinetic scheme, which is a standard technique in classical partial differential equations for illustrating the consistency of a numerical scheme as well as the dissipation and dispersion features [31,32]. For example, Jin and Levermore applied the asymptotic expansion to some semidiscrete (in space) schemes for hyperbolic systems with stiff relaxations [27], and then derived the so-called asymptotic modified equations (AME) corresponding to the limiting numerical schemes, from which the asymptotic properties were investigated by evaluating the leading order term in the truncation error under different scalings of the mesh size with respect to the relaxation parameter. Lowrie and Morel further analyzed the influence of high-order terms in the truncation error in the AME on the AP properties [15]. A similar method was also employed to analyze the time asymptotics of a class of IMEX Runge-Kutta schemes at the compressible Navier-Stokes level [23]. It is clearly shown that the modified equation approach can reveal the influence of scalings of mesh size (or time step) on the asymptotic behavior.

With the above understandings and motivated by the previous studies, in this article we attempt to present a clear picture of the *asymptotic process* for fully transport-collision coupled discrete kinetic schemes at small but nonzero Knudsen number, through the modified equation approach, aiming to provide the insight into the behavior of numerical solutions at small but nonzero numerical sizes. Specifically, we will introduce a new concept of *unified preserving* (UP) property, which is able to assess orders of asymptotics and the limiting equations underlying the scheme at small Knudsen numbers. This concept is motivated by the Taylor expansion analysis which can be employed to asses the degree of approximation between two functions. Given two functions $g(x)$ and $h(x)$ with sufficient smoothness, the Taylor series of them at $x=0$ can be expressed as $g(x)=\sum_{k=0}^{\infty} g^{(k)}x^k/k!$ and $h(x)=\sum_{k=0}^{\infty} h^{(k)}x^k/k!$, where $g^{(k)}$ and $h^{(k)}$ are the kth derivative of g and h evaluated at the point $x=0$, respectively. Then if $g^{(k)}=h^{(k)}$ for $k=0\sim n$, but $g^{(n+1)}\neq h^{(n+1)}$, we can say $g(x)$ and $h(x)$ are consistent with each other up to order n. Borrowing this idea, we define the UP property of a kinetic scheme to assess the approximation degree of f_h to f in terms of their Chapman-Enskog expansions. Specifically, if f_h can be expanded as $f_h(\epsilon;\Delta x,\Delta t;\boldsymbol{x},t)=\sum_{k=0}^{\infty}\epsilon^k f_h^{(k)}(\Delta x,\Delta t;\boldsymbol{x},t)$, then we can estimate the consistency between f_h and f by comparing the expansion coefficients $f^{(k)}$ and $f_h^{(k)}$ for $k=0,1,\cdots$, such that the approximation order of f_h to f can be determined. Since f is consistent with the hydrodynamic equations for small ϵ, it is expected that a consistent numerical solution of certain hydrodynamic equations can be extracted from f_h, depending on the approximation order of f_h to f. Particularly, at the leading order, f_h can give a numerical solution consistent with the Euler equations, or in other words, the kinetic scheme reduces to a numerical scheme for the Euler equations as $\epsilon\to 0$. In this regard, the UP concept is consistent with AP. But at higher orders, it can distinguish the hydrodynamic behaviors beyond the Euler limit, as those by the Chapman-Enskog analysis of the Boltzmann equation. Therefore, the UP concept is a generalization of AP, in the sense that it can not only be used to asses the hydrodynamic behaviors of a kinetic scheme at the Euler limit but also can provide its high-order hydrodynamics and estimate the order of asymptotics.

The paper is organized as follows. We summarize the kinetic equation and its asymptotic behavior at small Knudsen number in Sec. II. The concept of unified preserving schemes is proposed and justified in Sec. III. As two examples, the discrete unified gas-kinetic scheme (DUGKS) and a second-order IMEX scheme are analyzed in Sec. IV to demonstrate their UP properties. A summary is given in Sec. VI. We also provide a UP analysis of a kinetic scheme with collisionless reconstruction of cell interface distribution function in the Appendix A to show its dynamic difference from the DUGKS in the hydrodynamic regime.

II. KINETIC EQUATION AND ASYMPTOTIC BEHAVIORS

In this section we first give a brief introduction of kinetic models and the asymptotic analysis method which will be used later in this work. Although these are standard and can be found in books, e.g., Refs. [33,34], essential details presented here will make the later analysis much clearer. For simplicity we consider the BGK equation for a monatomic gas without external force (the same analysis should apply for general cases),

$$\partial_{\hat{t}}\hat{f}+\hat{\boldsymbol{\xi}}\cdot\hat{\boldsymbol{\nabla}}\hat{f}=\hat{Q}, \tag{1}$$

where $\partial_{\hat{t}}=\partial/\partial\hat{t}$ and $\hat{\boldsymbol{\nabla}}=\partial/\partial\hat{\boldsymbol{x}}$, $f(\hat{\boldsymbol{x}},\hat{\boldsymbol{\xi}},\hat{t})$ is the distribution function at time $\hat{t}$ and position $\hat{\boldsymbol{x}}$ for particles moving with velocity $\hat{\boldsymbol{\xi}}$, and the collision operator is

$$\hat{Q}=-\frac{1}{\hat{\tau}}(\hat{f}-\hat{f}^{(\mathrm{eq})}), \tag{2}$$

with $\hat{\tau}$ being the relaxation time which depends on the pressure and viscosity coefficient, and $\hat{f}^{(\mathrm{eq})}$ is the local Maxwellian equilibrium defined by the hydrodynamic variables $\hat{\boldsymbol{W}}=(\hat{\rho},\hat{\boldsymbol{u}},\hat{T})^T$,

$$\hat{f}^{(\mathrm{eq})}(\hat{\boldsymbol{W}})=\frac{\hat{\rho}}{(2\pi R\hat{T})^{D/2}}\exp\left(-\frac{|\hat{\boldsymbol{\xi}}-\hat{\boldsymbol{u}}|^2}{2R\hat{T}}\right), \tag{3}$$

where D is the spatial dimension, R is gas constant, while $\hat{\rho}$, $\hat{\boldsymbol{u}}$, and $\hat{T}$ are the gas density, velocity and temperature, respectively,

$$\hat{\boldsymbol{W}}=\begin{pmatrix}\hat{\rho}\\ \hat{\boldsymbol{u}}\\ \hat{T}\end{pmatrix}=\begin{pmatrix}\int\hat{f}\,d\hat{\boldsymbol{\xi}}\\ \frac{1}{\hat{\rho}}\int\hat{\boldsymbol{\xi}}\hat{f}\,d\hat{\boldsymbol{\xi}}\\ \frac{1}{D\hat{\rho}R}\int|\hat{\boldsymbol{\xi}}-\hat{\boldsymbol{u}}|^2\hat{f}\,d\hat{\boldsymbol{\xi}}\end{pmatrix}. \tag{4}$$

Note that the BGK operator is collisional invariant, i.e.,

$$\int\hat{Q}\,d\hat{\boldsymbol{\xi}}=0,\quad \int\hat{\boldsymbol{\xi}}\hat{Q}\,d\hat{\boldsymbol{\xi}}=\boldsymbol{0},\quad \int|\hat{\boldsymbol{\xi}}|^2\hat{Q}\,d\hat{\boldsymbol{\xi}}=0. \tag{5}$$

The asymptotic behavior of the kinetic Eq. (1) can be analyzed by the Chapman-Enskog expansion method in terms of the small parameter ϵ, proportional to the nondimensional Knudsen number introduced below, to relate with hydrodynamics [33]. For this purpose we first rewrite the BGK Eq. (1)

in a nondimensional form by introducing the following dimensionless variables,

$$\rho = \frac{\hat{\rho}}{\hat{\rho}_0}, \quad \boldsymbol{u} = \frac{\hat{\boldsymbol{u}}}{\hat{c}_0}, \quad T = \frac{\hat{T}}{\hat{T}_0}, \quad f = \frac{\hat{f}}{\hat{\rho}_0/\hat{c}_0^D}, \quad \boldsymbol{x} = \frac{\hat{\boldsymbol{x}}}{\hat{l}_0},$$
$$t = \frac{\hat{t}}{\hat{t}_0}, \quad \boldsymbol{\xi} = \frac{\hat{\boldsymbol{\xi}}}{\hat{c}_0}, \quad \tau = \frac{\hat{\tau}}{\hat{\tau}_0}, \tag{6}$$

where $\hat{\rho}_0$, $\hat{T}_0$ and $\hat{c}_0 = \sqrt{2R\hat{T}_0}$ are the reference density, temperature, and molecular velocity, respectively, while $\hat{l}_0$, $\hat{t}_0 = \hat{l}_0/\hat{c}_0$, and $\hat{\tau}_0$ are the reference length, time, and mean free time, respectively. It is noted that the relaxation time and mean free path can be related to the dynamic viscosity $\hat{\mu}$ and pressure $\hat{p} = \hat{\rho}R\hat{T}$ [34], namely, $\hat{\tau} = \hat{\mu}/\hat{p}$ and $\hat{\lambda} = \hat{\tau}\sqrt{\pi R\hat{T}/2}$, therefore the parameter $\epsilon = \hat{\tau}_0/\hat{t}_0 = \hat{\lambda}_0/\hat{l}_0$ (here $\hat{\lambda}_0 = \hat{c}_0\hat{\tau}_0$) is proportional to the Knudsen number Kn with the same order, which measures the ratio between the kinetic scale $(\hat{\tau}_0, \hat{\lambda}_0)$ and the hydrodynamic scale $(\hat{t}_0, \hat{l}_0)$. The dimensionless form of Eq. (1) can then be expressed as

$$\partial_t f + \boldsymbol{\xi}\cdot\nabla f = -\frac{1}{\epsilon}Q = -\frac{1}{\epsilon\tau}[f - f^{(\mathrm{eq})}(\rho, \boldsymbol{u}, T)], \tag{7}$$

where

$$f^{(\mathrm{eq})} = \frac{\rho}{(2\pi R_0 T)^{D/2}} \exp\left(-\frac{|\boldsymbol{\xi}-\boldsymbol{u}|^2}{2R_0T}\right), \quad (R_0 = 1/2). \tag{8}$$

In addition to the physical variables $\boldsymbol{x}$, t, and $\boldsymbol{\xi}$, the solution of Eq. (7) also depends on the parameter ϵ, i.e., $f = f(\epsilon; \boldsymbol{x}, \boldsymbol{\xi}, t)$. In the Chapman-Enskog analysis, it is assumed that the distribution function depends on space and time only through a functional dependence on the hydrodynamic variables, i.e., $f(\boldsymbol{x}, \boldsymbol{\xi}, t) = f(\boldsymbol{\xi}, \boldsymbol{W}(\boldsymbol{x}, t), \nabla\boldsymbol{W}(\boldsymbol{x}, t), \nabla\nabla\boldsymbol{W}(\boldsymbol{x}, t), \cdots)$. Under such assumption, the distribution function can be expressed as a series expansion in powers of ϵ [34],

$$f = f^{(0)} + \epsilon f^{(1)} + \epsilon^2 f^{(2)} + \cdots, \tag{9}$$

where the expansion coefficients $f^{(k)}$ depend on the hydrodynamic variables $\boldsymbol{W}$ and their gradients, with the assumption that $f^{(\mathrm{eq})} = O(1)$ and $f^{(k)} = O(1)$ for $k \geqslant 0$. Correspondingly, the time derivative is also expanded formally as a series of ϵ,

$$\partial_t = \partial_{t_0} + \epsilon\partial_{t_1} + \epsilon^2\partial_{t_2} + \cdots, \tag{10}$$

where ∂_{t_k} denotes the contribution to ∂_t from the spatial gradients of the hydrodynamic variables [33,34]. Specifically, the perturbation expansion (9) generates similar expansions of the pressure tensor and heat flux in the hydrodynamic balance equations, and ∂_{t_k} is defined to balance these terms at different orders of ϵ. In general, ∂_{t_k} is related to the $(k+1)$-order spatial gradients of the hydrodynamic variables.

The expansion coefficients $f^{(k)}$ can be found by substituting the above expansions into Eq. (7) and multiplying ϵ on both sides, which gives that

$$\epsilon^0: \quad f^{(0)} = f^{(\mathrm{eq})}, \tag{11a}$$

$$\epsilon^1: \quad D_0 f^{(0)} = -\frac{1}{\tau}f^{(1)}, \tag{11b}$$

$$\epsilon^2: \quad \partial_{t_1} f^{(0)} + D_0 f^{(1)} = -\frac{1}{\tau}f^{(2)}, \tag{11c}$$

$$\cdots\cdots \tag{11d}$$

$$\epsilon^k: \quad \sum_{j=1}^{k-1} \partial_{t_j} f^{(k-j-1)} + D_0 f^{(k-1)} = -\frac{1}{\tau}f^{(k)}, \tag{11e}$$

where $D_0 = \partial_{t_0} + \boldsymbol{\xi}\cdot\nabla$. In this work, we call the equations at different orders of ϵ as *balance equations*, which connect the coefficient $f^{(k)}$ to low-order ones from $f^{(0)}$ to $f^{(k-1)}$. Noting that with the conservation property (5) of the collision operator, we have

$$\int \boldsymbol{\psi} f^{(k)}\, d\boldsymbol{\xi} = 0, \quad k > 0, \tag{12}$$

where $\boldsymbol{\psi} = (1, \boldsymbol{\xi}, |\boldsymbol{\xi}|^2/2)$ are the collision invariants. Then the hydrodynamic equations can be derived with different approximation orders of ϵ. For instance, taking the conservative moments of Eq. (11b) leads to

$$\partial_{t_0}\int \boldsymbol{\psi} f^{(0)}\, d\boldsymbol{\xi} + \nabla\cdot\int \boldsymbol{\xi}\boldsymbol{\psi} f^{(0)}\, d\boldsymbol{\xi} = 0. \tag{13}$$

Since $f^{(0)} = f^{(\mathrm{eq})}$ as given in Eq. (11b), the equations can be rewritten as

$$\partial_{t_0}\rho + \nabla\cdot(\rho\boldsymbol{u}) = 0, \tag{14a}$$

$$\partial_{t_0}(\rho\boldsymbol{u}) + \nabla\cdot(\rho\boldsymbol{u}\boldsymbol{u} + p\boldsymbol{I}) = 0, \tag{14b}$$

$$\partial_{t_0}(\rho E) + \nabla\cdot[(\rho E + p)\boldsymbol{u}] = 0, \tag{14c}$$

where $\boldsymbol{I}$ is the second-order unit tensor, $p = \rho R_0 T$ is the dimensionless pressure and $E = c_v T + \frac{1}{2}|\boldsymbol{u}|^2$ is the dimensionless total energy with $c_v = DR_0/2$, which are just the Euler equations when we take the first-order approximation, i.e., $\partial_t = \partial_{t_0}$.

If we further take the conservative moments of Eq. (11c), then we can obtain

$$\partial_{t_1}\rho = 0, \tag{15a}$$

$$\partial_{t_1}(\rho\boldsymbol{u}) + \nabla\cdot\boldsymbol{P}^{(1)} = 0, \tag{15b}$$

$$\partial_{t_1}(\rho E) + \nabla\cdot\boldsymbol{Q}^{(1)} = 0, \tag{15c}$$

where $\boldsymbol{P}^{(1)} = \int \boldsymbol{\xi}\boldsymbol{\xi} f^{(1)}\, d\boldsymbol{\xi}$ and $\boldsymbol{Q}^{(1)} = \frac{1}{2}\int |\boldsymbol{\xi}|^2\boldsymbol{\xi} f^{(1)}\, d\boldsymbol{\xi}$. From Eq. (11b), we can evaluate the second-order tensor $\boldsymbol{P}^{(1)}$ and the vector $\boldsymbol{Q}^{(1)}$ explicitly,

$$-\frac{1}{\tau}P^{(1)}_{\alpha\beta} = \partial_{t_0}(\rho u_\alpha u_\beta + p\delta_{\alpha\beta}) + \nabla_\gamma \Gamma^{(0)}_{\alpha\beta\gamma}, \tag{16a}$$

$$-\frac{1}{\tau}Q^{(1)}_\alpha = \partial_{t_0}[(p+\rho E)u_\alpha] + \nabla_\beta \Theta^{(0)}_{\alpha\beta}, \tag{16b}$$

where $\boldsymbol{\Gamma}^{(0)} = \int \boldsymbol{\xi}\boldsymbol{\xi}\boldsymbol{\xi} f^{(0)}\, d\boldsymbol{\xi}$ and $\boldsymbol{\Theta}^{(0)} = \frac{1}{2}\int |\boldsymbol{\xi}|^2\boldsymbol{\xi}\boldsymbol{\xi} f^{(0)}\, d\boldsymbol{\xi}$. The time derivatives of ∂_{t_0} can be evaluated from Eq. (14), and after some standard algebra we can obtain that

$$P^{(1)}_{\alpha\beta} = -\sigma_{\alpha\beta} \equiv -\mu\left[\partial_\alpha u_\beta + \partial_\beta u_\alpha - \frac{2}{D}(\nabla\cdot\boldsymbol{u})\delta_{\alpha\beta}\right], \tag{17a}$$

$$Q^{(1)}_\alpha = -\kappa\partial_\alpha T - u_\beta\sigma_{\alpha\beta}, \tag{17b}$$

where $\mu = \tau p$ and $\kappa = \tau p(D+2)R_0/2$. Then with Eqs. (14) and (15), we obtain the hydrodynamic equations up to ϵ, i.e.,

$\partial_t = \partial_{t_0} + \epsilon\partial_{t_1}$,

$$\partial_t \rho + \nabla \cdot (\rho \boldsymbol{u}) = 0, \tag{18a}$$

$$\partial_t (\rho \boldsymbol{u}) + \nabla \cdot (\rho \boldsymbol{u}\boldsymbol{u} + p\boldsymbol{I}) = \nabla \cdot (\epsilon \boldsymbol{\sigma}), \tag{18b}$$

$$\partial_t (\rho E) + \nabla \cdot [(\rho E + p)\boldsymbol{u}] = \nabla \cdot (\epsilon \kappa T) + \nabla \cdot (\epsilon \boldsymbol{\sigma} \cdot \boldsymbol{u}), \tag{18c}$$

which are exactly the Navier-Stokes equations with a unit Prandtl number. The high-order hydrodynamic equations, such as the Burnett and super-Burnett equations, can be derived by invoking the corresponding high-order kinetic equations in the successive system (11).

Although the Chapman-Enskog expansion method is criticized from different viewpoints [35], it is still a useful approach to analyze the asymptotic behavior of kinetic models at small ϵ. Particularly, the Euler and Navier-Stokes equations derived from the kinetic model can precisely describe the corresponding hydrodynamic behaviors of the kinetic model. The higher-order hydrodynamic equations obtained from the Chapman-Enskog expansions usually suffer from physical and numerical difficulties. To overcome this defect, some modified versions of the Chapman-Enskog expansion have been proposed, such as the regularization one [36], the renormalization one [37], and the exact summation one [38]. With these reformulated Chapman-Enskog expansions, hydrodynamic equations with desired physics can be derived from the kinetic equation at higher orders, and it is now recognized that "*the problem with the Chapman-Enskog expansion is not the expansion itself but its truncation*" [39]. Therefore, the Chapman-Enskog expansion can still serve as a basis for analyzing the asymptotic behaviors of kinetic models as well as kinetic schemes. For simplicity, in the present work we will adopt the original Chapman-Enskog expansion method to illustrate the basic idea, but the analysis procedure presented here can also be conducted based on the modified versions. Furthermore, we note that high-order Chapman-Enskog analysis beyond the Navier-Stokes order is also helpful for designing kinetic schemes. For example, some lattice Boltzmann models incorporating the Burnett effect have been developed for two-phase flows with better performance [40], and a gas-kinetic scheme at the Burnett level has been developed for gas flows in slip regime [41].

III. DEFINITION OF UNIFIED PRESERVING (UP) PROPERTY

A numerical scheme for the kinetic Eq. (7), denoted by P_h^ϵ, gives an approximate distribution function f_h, depending on the cell size Δx and time step Δt, i.e., $f_h = f_h(\epsilon; \boldsymbol{x}, \boldsymbol{\xi}, t; \Delta x, \Delta t)$. Therefore, it is expected that the asymptotic behavior of P_h^ϵ depends not only on the kinetic and hydrodynamics scales, but also on the numerical scale $h = (\Delta x, \Delta t)$ (or $\Delta\hat{\boldsymbol{x}}$ and $\Delta\hat{t}$ in dimensional form). It is noted that we concentrate here on the time and space discretizations while the velocity discretization is not considered in this work. Furthermore, we assume that the cell size and time step are adequate to resolve the flow physics at the hydrodynamic scale, similar to many Navier-Stokes solvers.

To assess the asymptotic property of P_h^ϵ at small ϵ on the hydrodynamic scale, we can again apply the Chapman-Enskog expansion to f_h,

$$f_h = f_h^{(0)} + \epsilon f_h^{(1)} + \epsilon^2 f_h^{(2)} + \cdots. \tag{19}$$

Then we compare the expansion coefficients $f_h^{(k)}$ with those of the original distribution function $f(\boldsymbol{x}, \boldsymbol{\xi}, t)$ given by Eq. (9). The comparison leads to the definition of *unified preserving* property of the kinetic scheme P_h^ϵ.

Definition 1. A consistent numerical scheme of Eq. (7), P_h^ϵ, is called an nth order *unified preserving* (UP) scheme provided that

(i) it is uniformly stable, i.e., the scheme is stable regardless of ϵ;

(ii) it is a legitimate discretization of the collisionless kinetic equation as $\epsilon \to \infty$;

(iii) for $\epsilon \ll 1$, there exist two parameters $\alpha_0 \in [0, 1)$ and $\beta_0 \in [0, 1)$, such that as $\Delta t = O(\epsilon^\alpha)$ and $\Delta x = O(\epsilon^\beta)$ with $\alpha_0 < \alpha < 1$ and $\beta_0 < \beta < 1$, the expansion coefficients and the associated discrete balance equations satisfy

$$f_h^{(0)} = f_h^{(\mathrm{eq})},$$

$$\sum_{j=1}^{k-1} \partial_t^{(j)} f_h^{(k-j-1)} + D_0 f_h^{(k-1)} = -\frac{1}{\tau} f_h^{(k)} \quad (1 \leqslant k \leqslant n), \tag{20}$$

but $f_h^{(n+1)}$ depends on Δx or Δt explicitly.

In the above definition, $f_h^{(\mathrm{eq})} = f^{(\mathrm{eq})}(\boldsymbol{W}_h)$ is the Maxwellian distribution function dependent on the numerical hydrodynamic variables $\boldsymbol{W}_h = (\rho_h, \boldsymbol{u}_h, T_h)^T$, which is defined as in Eq. (4) with f being replaced by f_h. The first (stable) condition suggests that the time step is not limited by the relaxation time in terms of numerical stability, which requires a nonexplicit treatment of the (stiff) collision term. The second condition suggests that the scheme can capture free transport of particles in the free molecular regime, which is essential for a multiscale kinetic scheme.

The third (asymptotic) condition indicates that the scheme can capture the hydrodynamic behaviors to some degree without resolving the kinetic scales. To see this more clearly, we introduce two parameters,

$$\delta_t \equiv \frac{\Delta t}{\epsilon} = \frac{\Delta \hat{t}}{\hat{\tau}_0}, \quad \delta_x \equiv \frac{\Delta x}{\epsilon} = \frac{\Delta \hat{x}}{\hat{\lambda}_0}, \tag{21}$$

which measure the numerical temporal and spatial resolutions of the kinetic scales. For sufficient small ϵ, it can be seen that $\delta_t = O(\epsilon^{\alpha-1}) \gg 1$ and $\delta_x = O(\epsilon^{\beta-1}) \gg 1$, meaning that the numerical scale is much larger than the kinetic scale. Furthermore, the condition $f_h^{(0)} = f_h^{(\mathrm{eq})}$ suggests that the discrete collision operator be also conservative, and therefore

$$\int \boldsymbol{\psi} f_h^{(k)}\, d\boldsymbol{\xi} = 0, \quad k > 0. \tag{22}$$

Then it can be seen that the second equation in Eq. (20) has the same property as Eq. (11e), and their moment equations are also identical for $1 \leqslant k \leqslant n$. For instance, for a first-order ($n = 1$) UP scheme, we have

$$D_0 f_h^{(0)} = -\frac{1}{\tau} f_h^{(1)}. \tag{23}$$

Taking conservative moments of the above equation leads to

$$\partial_{t_0}\rho_h + \nabla\cdot(\rho_h \boldsymbol{u}_h) = 0, \tag{24a}$$

$$\partial_{t_0}(\rho_h \boldsymbol{u}_h) + \nabla\cdot(\rho_h \boldsymbol{u}_h\boldsymbol{u}_h + p_h \boldsymbol{I}) = 0, \tag{24b}$$

$$\partial_{t_0}(\rho_h E_h) + \nabla\cdot[(\rho_h E_h + p_h)\boldsymbol{u}_h] = 0, \tag{24c}$$

where $p_h = \rho_h R_0 T_h$ and $E_h = c_v T_h + \frac{1}{2}|\boldsymbol{u}_h|^2$. It can be seen that Eqs. (24) are the same as those of the original BGK equation at the Euler level [see Eqs. (14)], which means that the numerical hydrodynamic quantities $\boldsymbol{W}_h$ are the solutions of the Euler equations. In other words, a first-order UP kinetic scheme can reproduce the Euler equations exactly with a coarse numerical resolution without resolving the kinetic scale, and this fact also indicates that the scheme has the AP properties. However, since the equation of a first-order UP scheme for $f_h^{(2)}$ is incomparable with that of $f^{(2)}$, the balance moment equations at ϵ^2 are different, such that the Navier-Stokes equations cannot be recovered from the scheme. Actually, to capture the hydrodynamic behaviors at the Navier-Stokes level, a second-order UP scheme is required. In this case, $f_h^{(1)}$ satisfies Eq. (23), and $f_h^{(2)}$ satisfies

$$\partial_{t_1} f_h^{(0)} + D_0 f_h^{(1)} = -\frac{1}{\tau} f_h^{(2)}, \tag{25}$$

which is the same as Eq. (11b), and the conservative moment equations take the same form as Eq. (15) together with Eq. (17a), with $\boldsymbol{W}$ being replaced by $\boldsymbol{W}_h$. As such, the numerical quantities $\boldsymbol{W}_h$ from the second-order UP scheme satisfy the Navier-Stokes equations. To proceed further, a third-order UP scheme can capture the hydrodynamic behaviors at the Burnett level, and a fourth-order one will go to the super-Burnett level. Generally, for an nth UP scheme, the expansion coefficients of $f_h^{(k)}$ satisfy the same equations of $f^{(k)}$ for $0 \leqslant k \leqslant n$, such that the hydrodynamic quantities $\boldsymbol{W}_h$ also satisfy the corresponding nth order hydrodynamic equations obtained from the Chapman-Enskog analysis of the original kinetic equation. Therefore, the concept of UP can be used to distinguish the asymptotic limiting equations of different kinetic schemes for small Knudsen numbers with different orders.

Remark 1. It should be noted that a UP scheme is a consistent discretization of the kinetic Eq. (1), and f_h is an approximation solution of the kinetic equation rather than the solution of the limiting hydrodynamic equations. Therefore, for relative large ϵ, f_h can still be a good approximation to the solution of the kinetic equation instead of the high-order hydrodynamic equations such as the Burnett or super-Burnett ones.

Remark 2. It is noted that $\Delta t = \delta_t \epsilon = \Delta\hat{t}/\hat{t}_0$ and $\Delta x = \delta_x \epsilon = \Delta\hat{x}/\hat{l}_0$, which represent the numerical time and mesh resolutions for the hydrodynamic scale. Generally, the numerical resolutions must resolve the hydrodynamic scale flow structure for hydrodynamic problems, i.e., $\Delta t < 1$ and $\Delta x < 1$, suggesting that $\alpha \geqslant 0$ and $\beta \geqslant 0$. Particularly, as $\alpha = 0$ and/or $\beta = 0$, we have $\delta_t = O(\epsilon^{-1})$ and/or $\delta_x = O(\epsilon^{-1})$, meaning that the kinetic time and/or length scales are unresolved, and this is referred to as "unresolved regime" in Ref. [15] or "thick regime" in Ref. [12]. However, this does not mean that the hydrodynamic scales are not resolved. Generally, if the flow exhibits certain hydrodynamic structure, the numerical resolutions should resolve the typical hydrodynamic scales to capture the flow structure, such as the hydrodynamic boundary layer.

The UP property of P_h^ϵ can be analyzed by studying the asymptotics of its modified (or equivalent) equation. We consider the one-dimensional case without loss of generality, then the modified equation of a numerical scheme for Eq. (7) can generally be expressed as

$$\partial_t f_h + \xi\,\partial_x f_h + O(\Delta t^s, \Delta x^q)\mathcal{L} f_h = \frac{1}{\epsilon} Q(f_h) + \frac{1}{\epsilon} O(\Delta t^r)\mathcal{L} Q_h, \tag{26}$$

where s, q, and r are the orders of the leading terms of the truncation errors for the temporal integration, spatial gradient discretization, and collision integration, respectively. Note that the time derivatives of f_h with orders higher than one can be eliminated by using the equation itself. Then substituting the Chapman-Enskog expansion of f_h given by Eq. (19) and the time expansion (10) into Eq. (26), one can obtain the set of successive equations of $f_h^{(k)}$ in terms of the order of ϵ. Note that we can substitute them successively in terms of ∂_x^q terms, which is just the same strategy as adopted in the modified equation approach [31,32].

Substituting the expansions (10) and (19) into the modified Eq. (26), together with the numerical scales $\Delta t = O(\epsilon^\alpha)$ and $\Delta x = O(\epsilon^\beta)$, we can obtain the expansion coefficients $f_h^{(k)}$ and the corresponding balance equations at different orders of ϵ. The UP order can then be determined by comparing $f_h^{(k)}$ with $f^{(k)}$. In general, for an nth order UP scheme, it is required that $\Delta t^s = o(\epsilon^{n-1})$, $\Delta t^r = o(\epsilon^{n-1})$, and $\Delta x^q = o(\epsilon^{n-1})$, since in this case the terms associated with Δx and Δt do not appear in the balance equations for $f_h^{(k)}$ for $0 \leqslant k \leqslant n$. This suggest that we can choose $\alpha_0 = \min[(n-1)/s, (n-1)/r]$ and $\beta_0 = (n-1)/q$ in the asymptotic condition for P_h^ϵ.

It is clear that the UP order of P_h^ϵ depends on not only the numerical scale $h = (\Delta x, \Delta t)$, but also the discretization accuracy (s, q, r). Physically, this indicates the capability of the scheme in resolving the flow physics depends on not only the numerical resolution (time step and grid spacing) or the grid Knudsen number $(1/\delta_x)$, as argued in Ref. [1], but also the accuracy of the scheme. In other words, for a given mesh size and time step the numerical flow physics can be different from different kinetic schemes with different accuracy.

The UP property of a kinetic scheme is illustrated in Fig. 1. The original kinetic equation with the small parameter ϵ is represented by P^ϵ, and P_h^ϵ is a consistent discretization of P^ϵ with numerical scale h, namely, $P_h^\epsilon \to P^\epsilon$ as $h \to 0$ (represented by the left downward arrow). $H^\infty(\epsilon) = \{f^{(k)} | 0 \leqslant k < \infty\}$ is the set of the Chapman-Enskog expansion coefficients of f defined by Eq. (11), which is determined from the kinetic equation P^ϵ at small ϵ (represented by the bottom rightward arrow). $H_h^n(\epsilon) = \{f_h^{(k)} | 0 \leqslant k \leqslant n\}$ is the set of the Chapman-Enskog expansion coefficients of f_h defined by Eq. (20), which is determined from the kinetic scheme P_h^ϵ at small ϵ (represented by the top rightward arrow). An nth order UP scheme means that $H_h^n(\epsilon)$ is a subset of $H^\infty(\epsilon)$ as $h \gg \epsilon$ and approaches to $H^\infty(\epsilon)$ closer with increasing n, which is represented by the right downward arrow. Note that $H^\infty(\epsilon)$ and $H_h^n(\epsilon)$ also determine uniquely the moment equations of the kinetic equation P^ϵ and the kinetic scheme $P_h^n(\epsilon)$ at different

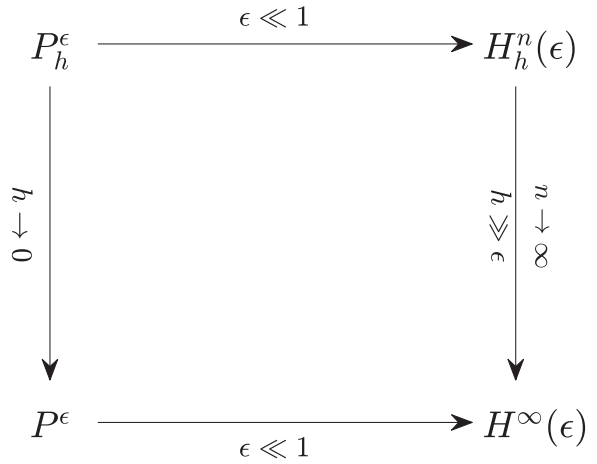

FIG. 1. Schematic diagram of a UP kinetic scheme of order n. Here P^ϵ is the kinetic equation, P_h^ϵ is a consistent kinetic scheme with discrete resolution h, $H^\infty(\epsilon)$ is the set of the Chapman-Enskog expansion coefficients of the solution of P^ϵ, and $H_h^k(\epsilon)$ is the set of the expansion coefficients of the solution of P_h^ϵ. For an nth order UP scheme, $f_h^{(k)} = f^{(k)}$ for $0 \leqslant k \leqslant n$.

orders of ϵ, respectively, and therefore the underlying moment equations of P_h^ϵ at orders of ϵ from 0 to n are the same as those of P^ϵ.

In addition to the function on the assessment of asymptotic orders, the UP concept also provides a picture how a kinetic scheme approaches to the asymptotic limit, as demonstrated in Fig. 2. In the classical AP concept, a kinetic scheme P_h^ϵ approaches to its discrete asymptotic limit P_h^0 first following the line of $h = O(\epsilon^0)$ (i.e., $\epsilon \to 0$ with fixed Δx and/or Δt),

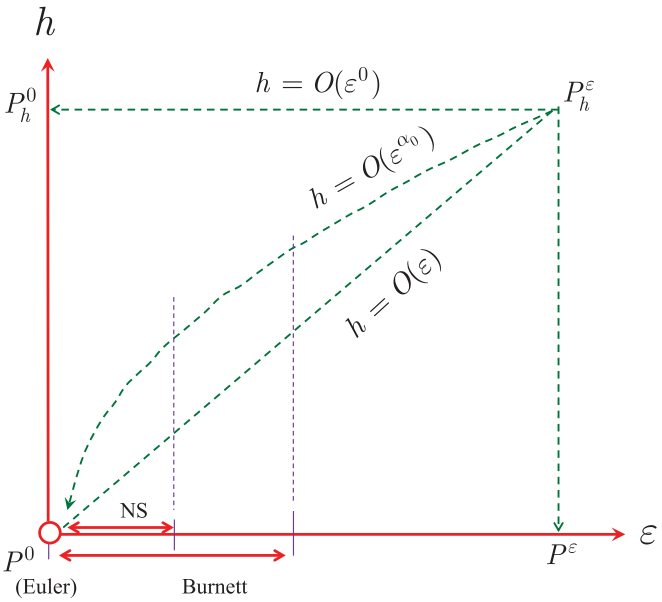

FIG. 2. Schematic diagram of the asymptotic path to the limiting hydrodynamic regimes. The region below the line $h = O(\epsilon)$ suggests resolved kinetic scale. The line $h = O(\epsilon^{\alpha_0})$ represents the upper limit for a UP scheme (or α_0 is the infimum of the set $\{\alpha\}$). The region between the two lines $h = O(\epsilon)$ and $h = O(\epsilon^{\alpha_0})$ represents the parameter space for a UP scheme.

and then approaches to the analytical limit P^0 following the h axis ($h \to 0$). This suggests that an asymptotic scheme may not pass the Navier-Stokes region, as demonstrated in Ref. [29] where an AP-IMEX scheme was shown to fail to capture the Navier-Stokes solution of a steady flow. However, a UP scheme of order higher than 2 can approach to the hydrodynamic limit passing through the Navier-Stokes regime following a curve below the line $h = O(\epsilon^{\alpha_0})$. Figure 2 also suggests that a smaller value of α_0 is preferred in designing multiscale kinetic schemes. In other words, a kinetic scheme with a smaller α_0 can capture the hydrodynamic behaviors with larger cell size and/or time step, and is thus will be more efficient. It is also noted that although a multiscale kinetic scheme with UP properties will pass the Burnett region, the temporal and spatial discretizations are usually less restrictive since the flow lies in the transition regime where the flow dynamics can be captured under coarse numerical scales.

We remark that the modified equation approach was also employed in some previous AP analysis, as noted in item (iii) of the introduction section. Particularly, Lowrie and Morel studied the asymptotics behavior of a certain space semidiscrete numerical scheme for hyperbolic systems with a stiff relaxation term [15], by applying the asymptotic expansion to the modified equation of the scheme. A so-called *asymptotic modified equation* (AME) is then derived from the multiscale expansion, which can be viewed as the modified equation for the limiting asymptotic equation. By examining the truncation error that may depend on the scaling parameter ϵ and mesh size Δx, the leading-order asymptotic behavior of the numerical scheme can be figured out. It was shown that the dimensionless parameter characterizing the near-equilibrium limit should be fixed to discriminate AP and non-AP schemes, and the high-order error terms in Δx dominate the AP property. The UP analysis shares some similarities with the above AME approach, in the sense that both analyze the asymptotic behavior of a numerical scheme by applying the asymptotic expansion to the modified equation. However, some discrepancies between the two approaches are also clear. First, the aim of the AME approach is to distinguish whether or not a scheme is AP for the leading-order solution in the limit of $\epsilon \to 0$, while the UP aims to figure out the asymptotic behaviors at different orders of ϵ, which presents more detailed AP information quantitatively. Second, in the AME approach the asymptotic modified equation corresponding to the numerical scheme for the limiting asymptotic equation is derived explicitly, from which the influence of the mesh size on the AP can be analyzed. However, in the UP analysis only the modified equation for the original numerical scheme (26) is presented, which is used only to derive the expansion coefficients (and the balance equation at each order), while the modified equation for the corresponding asymptotic numerical scheme does not appear. Finally, unlike the UP analysis, in the AME approach the numerical solution (f_h) is not distinguished from the solution of the original continuous equation (f), which may lead to some confusions between their asymptotic behaviors.

It is noted that the discrete Chapman-Enskog expansion was also adopted in some previous studies on time asymptotics of certain semidiscrete kinetic schemes, e.g., Refs. [5,18,19,23,24]. However, the analysis in these studies

focused on time asymptotics where the spatial gradient of the scheme was assumed to be exact. As will be shown later in the UP analysis of several example kinetic schemes, the spatial discretization plays a key role for their aysmptotic behaviors, which means the sole time asymptotic analysis is insufficient for evaluating the overall behaviors at different hydrodynamic levels. This is reasonable since the temporal-spatial coupling reflects the real physics underlying the kinetic equation. Furthermore, in these studies the Chapman-Enskog approximation of the discrete distribution function was substituted into the numerical scheme. The analysis shows that the moments of the numerical scheme are just certain discretization formulations of the corresponding hydrodynamic equations. However, the Chapman-Enskog expansion of the numerical solution in the UP analysis is applied to the modified equation, such that the hydrodynamic equations underlying the schemes with different numerical resolutions can be revealed, which are unavailable in the former approach.

Finally, it is interesting to compare the present UP analysis with the multiscale expansion (ME) method for lattice Boltzmann equation (LBE) (e.g., Ref. [42]), which is widely used for analyzing the hydrodynamic behaviors of LBE. As noted above, in the UP analysis three scale levels are involved, i.e., kinetic scales $(\hat{\lambda}_0, \hat{\tau}_0)$, numerical scales $(\Delta\hat{\boldsymbol{x}}, \Delta\hat{t})$, and hydrodynamics scales $(\hat{l}_0, \hat{t}_0)$. The hydrodynamic behaviors of a kinetic scheme depend not only on the kinetic and hydrodynamic scales, measured by the Knudsen number ϵ as the scaling parameter, but also on the numerical scales. However, in the ME analysis [42], the LBE is just viewed as a kinetic model similar to the continuous Boltzmann equation, in which the lattice time step and lattice spacing are taken as the collision time and mean-free path. In other words, in LBE the numerical scales are the same as kinetic scales. This is also evident from the definition of the scaling parameter ($\epsilon = \Delta x \equiv \Delta\hat{\boldsymbol{x}}/\hat{l}_0$) used in the expansion, which is clearly different from the Knudsen number used in the UP analysis. The aim of the multiscale analysis of LBE is to show its hydrodynamic behaviors, just as the original Chapman-Enskog or asymptotic analysis for the continuous Boltzmann equation. Therefore, in the multiscale analysis used for LBE, the physical kinetic scales, $\hat{\lambda}$ and $\hat{\tau}$, are not considered, and the influences of $\Delta\hat{\boldsymbol{x}}/\hat{\lambda}_0$ and $\Delta\hat{t}/\hat{\tau}_0$ on hydrodynamics cannot be identified.

IV. EXAMPLE I: UP PROPERTIES OF DUGKS

In this section, we will take the discrete unified gas-kinetic scheme (DUGKS) [7] as an example to show how the UP properties are analyzed.

A. Formulation of DUGKS

The DUGKS is a finite-volume discretization of the kinetic Eq. (7) for simulating gas flows in all regimes. For simplicity, we will consider the one-dimensional case, and the flow is assumed to be isothermal and smooth without shock discontinuities with a constant relaxation time τ. The computational domain will be divided into a number of uniform cells centered at x_j $(j = 1, 2, \cdots, N)$ with cell size Δx, and the interface between cell j and $j+1$ is denote by $x_{j+1/2}$. The DUGKS can then be expressed as

$$\frac{f_j^{n+1} - f_j^n}{\Delta t} + \xi \frac{f_{j+1/2}^{n+1/2} - f_{j-1/2}^{n+1/2}}{\Delta x} = \frac{1}{2\epsilon}\left[Q_j^n + Q_j^{n+1}\right], \quad (27)$$

where $f_j^n = f_h(x_j, \xi, t_n)$ is the cell-averaged numerical solution over the cell centered at x_j at time $t_n = n\Delta t$, and $Q_j^n = Q_h(x_j, \xi, t_n) = -\frac{1}{\tau}[f_h(x_j, \xi, t_n) - f_h^{(\mathrm{eq})}(x_j, \xi, t_n)]$ is the corresponding cell-averaged numerical collision term. Note that here the mid-point and trapezoidal quadrature rules are applied to the convection and collision terms, respectively. The distribution function at cell interface at the half time step $f_{j+1/2}^{n+1/2} = f_h(x_{j+1/2}, \xi, t_n + \Delta t/2)$ is reconstructed by integrating the kinetic equation along the characteristic line with a half time step,

$$f_{j+1/2}^{n+1/2} - f_{j'}^n = \frac{1}{2\epsilon}\left[Q_{j'}^n + Q_{j+1/2}^{n+1/2}\right], \quad (28)$$

where $f_{j'}^n = f_h(x_{j+1/2} - \xi\Delta t/2, t_n)$ is the distribution function at the starting point. Note that the implicit discretization in Eqs. (27) and (28) can be removed by introducing two auxiliary distribution functions in practical computations [7]. In DUGKS, $f_{j'}^n$ is linearly interpolated from the cell-center distribution function,

$$f_{j'}^n = f_{j+1/2}^n - \frac{\Delta t}{2}\xi\sigma_{j+1/2}^n, \quad (29)$$

where $\sigma_{j+1/2}^n$ is the slope. For smooth flows, the following approximation can be employed,

$$f_{j+1/2}^n = \frac{f_j^n + f_{j+1}^n}{2}, \quad \sigma_{j+1/2}^n = \frac{f_{j+1}^n - f_j^n}{\Delta x}. \quad (30)$$

$Q_{j'}^n$ in Eq. (28) can be obtained similarly. Then from Eq. (28), $f_{j+1/2}^{n+1/2}$ can be expressed as

$$f_{j+1/2}^{n+1/2} = \left(\frac{1}{2} - \beta\right)\left[f_{j+1}^n + \frac{\Delta t}{4\epsilon}Q_{j+1}^n\right] + \left(\frac{1}{2} + \beta\right)\left[f_j^n + \frac{\Delta t}{4\epsilon}Q_j^n\right] + \frac{\Delta t}{4\epsilon}Q_{j+1/2}^{n+1/2}, \quad (31)$$

where $\beta = \frac{1}{2}\xi\Delta t/\Delta x$.

B. Uniform stability

Regarding the numerical stability of DUGKS, it is not a main task of the present work to give a rigorous analysis. Hence, it is just estimated *heuristically* as follows. First, since the collision term in DUGKS [see Eqs. (27) and (31)] is integrated with the trapezoidal rule, which is a semi-implicit time discretization, roughly the small parameter ϵ in the collision term has no direct influence on the time step. Indeed, we can think DUGKS as the average of the explicit and the implicit schemes,

$$\frac{f_j^{n+1} - f_j^n}{\Delta t} + \xi \frac{f_{j+\frac{1}{2}}^n - f_{j-\frac{1}{2}}^n}{\Delta x} = \frac{1}{\epsilon}Q_j^n, \quad (32)$$

$$\frac{f_j^{n+1} - f_j^n}{\Delta t} + \xi \frac{f_{j+\frac{1}{2}}^{n+1} - f_{j-\frac{1}{2}}^{n+1}}{\Delta x} = \frac{1}{\epsilon}Q_j^{n+1}, \quad (33)$$

$$f_{j+\frac{1}{2}}^{n+\frac{1}{2}} = \frac{1}{2}\left(f_{j+\frac{1}{2}}^n + f_{j+\frac{1}{2}}^{n+1}\right) + O(\Delta t^2). \quad (34)$$

Then DUGKS is equivalent to the Crank-Nicolson type discretization of Eq. (1) within second-order accuracy, being equipped with the IMEX character. As is well-known that the Crank-Nicolson type discretization is unconditional stable, so is DUGKS as demonstrated by a number of numerical results in previous studies [30], although the convection CFL constraint,

$$\Delta t \leqslant \frac{\eta \Delta x}{|\xi|_{\max}}, \tag{35}$$

is still required theoretically because of the interaction of transport and collision, where $0 < \eta < \eta_0$ is the CFL number and $|\xi|_{\max}$ is the maximum discretized particle velocity, η_0 is some constant.

We just point out that DUGKS has the characteristic of Lax-Wendroff type schemes, thanks to Eq. (28) or Eq. (31) that has the implication of temporal-spatial coupling. This is evident in the analysis in Sec. IV D below.

C. Collisionless limit

In the collisionless limit as $\epsilon \to \infty$, from Eq. (31) we can obtain the cell-interface distribution function at half time step,

$$f_{j+1/2}^{n+1/2} = \frac{1}{2}\left(f_j^n + f_{j+1}^n\right) - \frac{\xi \Delta t}{2\Delta x}\left(f_{j+1}^n - f_j^n\right), \tag{36}$$

and the DUGKS (27) becomes

$$\frac{f_j^{n+1} - f_j^n}{\Delta t} + \frac{\xi}{2\Delta x}\left(f_{j+1}^n - f_{j-1}^n\right) - \frac{\xi^2 \Delta t}{2\Delta x^2}\left(f_{j+1}^n - 2f_j^n + f_{j-1}^n\right) = 0, \tag{37}$$

which is just the Lax-Wendroff scheme for the collisionless BGK equation. This means that the DUGKS is a legitimate scheme in the limit $\epsilon \to \infty$, and the stability condition is

$$\frac{|\xi|_{\max} \Delta t}{\Delta x} \leqslant 1, \tag{38}$$

which is consistent with the CFL condition (35).

D. Modified equation analysis

To obtain the modified equation of the DUGKS, we first perform Taylor expansions of $f_{j\pm1/2}^{n+1/2}$ defined by Eq. (31) at $(x, t) = (x_j, t_n)$, leading to the following equation after some standard algebraic manipulations,

$$\begin{aligned}
&\frac{f_{j+1/2}^{n+1/2} - f_{j-1/2}^{n+1/2}}{\Delta x} \\
&= \partial_x f_h + \frac{\Delta x^2}{6}\partial_x^3 f_h - \frac{\Delta t}{2}\xi \partial_x^2 f_h + \frac{\Delta t}{2\epsilon}\partial_x Q_h \\
&\quad - \frac{1}{2\epsilon}\left(\frac{\Delta t}{2}\right)^2 \xi \partial_x^2 Q_h + \frac{1}{2\epsilon}\left(\frac{\Delta t}{2}\right)^2 \partial_x \partial_t Q_h \\
&\quad + O(\Delta t^3, \Delta t \Delta x^2)\mathcal{L}\left(\frac{1}{\epsilon}Q_h\right) + O(\Delta x^3, \Delta t \Delta x^2)\mathcal{L} f_h,
\end{aligned} \tag{39}$$

where $\mathcal{L}(\cdot)$ is a general linear operator acting on the dummy variable, representing the collection of temporal and spatial derivatives of different orders. It can take different forms at different places. Here and below we ignore the difference when no confusion is caused. The prefactor in the front of $\mathcal{L}$ denotes the corresponding leading orders in Δx and Δt in the collection. Note that the collision term also appears in the discretization of the flux, which is a special feature of DUGKS and implies that both the transport and collision effects of particles be precisely included in the scheme. With the above result and performing Taylor expansions of other two terms in Eq. (27) at t_n, we can obtain that

$$\begin{aligned}
&\partial_t f_h + \xi \partial_x f_h + \frac{\Delta t}{2}\underbrace{\left[\partial_t^2 f_h - \xi^2 \partial_x^2 f_h - \frac{1}{\epsilon}\partial_t Q_h + \frac{1}{\epsilon}\xi \partial_x Q_h\right]}_{A} \\
&\quad + \frac{\Delta t^2}{6}\underbrace{\left[\partial_t^3 f_h + \frac{3}{4\epsilon}\left(\xi \partial_x \partial_t Q_h - \xi^2 \partial_x^2 Q_h - 2\partial_t^2 Q_h\right)\right]}_{B} \\
&\quad + \frac{\Delta x^2}{6}\xi \partial_x^3 f_h \\
&= \frac{1}{\epsilon}Q_h + O(\Delta t^3, \Delta t \Delta x^2)\mathcal{L}\left(\frac{1}{\epsilon}Q_h\right) \\
&\quad + O(\Delta x^3, \Delta t \Delta x^2, \Delta t^3)\mathcal{L} f_h.
\end{aligned} \tag{40}$$

The high-order time derivatives of f_h can be replaced in terms of spatial derivatives successively using Eq. (40), as done in the modified equation approach [31]. We will discuss this below.

For the underbraced term A, we can obtain by making use of Eq. (40) that

$$\begin{aligned}
A &= (\partial_t - \xi \partial_x)\left(\partial_t f_h + \xi \partial_x f_h - \frac{1}{\epsilon}Q_h\right) \\
&= -\frac{\Delta t}{2}(\partial_t - \xi \partial_x)A + O(\Delta t^2)\mathcal{L}\left(\frac{1}{\epsilon}Q_h\right) \\
&\quad + O(\Delta x^2, \Delta t^2)\mathcal{L} f_h,
\end{aligned} \tag{41}$$

which gives that

$$A = O(\Delta t^2)\mathcal{L}\left(\frac{1}{\epsilon}Q_h\right) + O(\Delta x^2, \Delta t^2)\mathcal{L} f_h. \tag{42}$$

Therefore, the modified Eq. (40) can be rewritten as

$$\partial_t f_h + \xi \partial_x f_h + \frac{\Delta t^2}{6}B + \frac{\Delta x^2}{6}\xi \partial_x^3 f_h = \frac{1}{\epsilon}Q_h + \text{HoT}, \tag{43}$$

where HoT is the sum of high-order terms,

$$\text{HoT} = O(\Delta t^3, \Delta t \Delta x^2)\mathcal{L}\left(\frac{1}{\epsilon}Q_h\right) + O(\Delta x^3, \Delta t \Delta x^2, \Delta t^3)\mathcal{L} f_h. \tag{44}$$

The first term in HoT contains the scaling parameter ϵ, but we will show below that it has the same order as the second term, and thus HoT depends only on Δt and Δx. To this end, we rewrite Eq. (43) as

$$\begin{aligned}
&[1 + O(\Delta t^2)\mathcal{L}]\left(\frac{1}{\epsilon}Q_h\right) \\
&= \partial_t f_h + \xi \partial_x f_h + \frac{\Delta t^2}{6}\partial_t^3 f_h \\
&\quad + \frac{\Delta x^2}{6}\xi \partial_x^3 f_h + O(\Delta x^3, \Delta t \Delta x^2, \Delta t^3)\mathcal{L} f_h,
\end{aligned} \tag{45}$$

suggesting that

$$\frac{Q_h}{\epsilon} = \partial_t f_h + \xi \partial_x f_h + O(\Delta x^2, \Delta t^2)\mathcal{L} f_h. \tag{46}$$

With this estimation, the underbraced term B in Eq. (40) can be rewritten as

$$B = -\tfrac{1}{2}\partial_t^3 f_h - \tfrac{3}{4}\xi^3 \partial_x^3 f_h - \tfrac{3}{4}\xi \partial_x \partial_t^2 f_h + O(\Delta x^2, \Delta t^2)\mathcal{L} f_h, \tag{47}$$

and HoT given by Eq. (44) is

$$\text{HoT} = O(\Delta x^3, \Delta t \Delta x^2, \Delta t^3)\mathcal{L} f_h = O(\Delta x^3, \Delta t \Delta x^2, \Delta t^3), \tag{48}$$

which is independent of ϵ. We will neglect $\mathcal{L} f_h$ in what follows for simplicity, since ϵ does not appear in these terms. Then the modified Eq. (40) can be rewritten as

$$\partial_t f_h + \xi \partial_x f_h + \frac{\Delta t^2}{6} B + \frac{\Delta x^2}{6} \xi \partial_x^3 f_h = \frac{1}{\epsilon} Q_h + O(\Delta x^3, \Delta t \Delta x^2, \Delta t^3). \tag{49}$$

It is clear that as $\Delta t \to 0$ and $\Delta x \to 0$, the modified Eq. (49) reduces to the kinetic Eq. (1), suggesting that the DUGKS consisting of Eqs. (27) and (31) is a consistent second-order scheme in both time and space for the BGK Eq. (7).

E. Asymptotic property

For the asymptotic property of DUGKS at small ϵ, we have the following result.

Theorem 1. As $\Delta t = O(\epsilon^\alpha)$ and $\Delta x = O(\epsilon^\beta)$ with $\alpha \in (0.5, 1)$ and $\beta \in (0.5, 1)$, the Chapman-Enskog expansion coefficients of f_h obtained from DUGKS satisfy Eq. (20) for $n = 2$ if the relaxation time τ is constant.

Proof. With the condition for Δt and Δx, we can write the modified Eq. (49) as

$$\epsilon \partial_t f_h + \epsilon \xi \partial_x f_h + \frac{a}{6}\epsilon^{2\alpha+1} B + \frac{b}{6}\epsilon^{2\beta+1}\xi \partial_x^3 f_h = Q_h + o(\epsilon^2), \tag{50}$$

where $a = O(1)$ and $b = O(1)$ are two constants. Substituting the Chapman-Enskog expansions (19) and (10) into the above equation leads to the successive equations in terms of the orders of ϵ.

Note that $2 < 2\alpha + 1 < 3$ and $2 < 2\beta + 1 < 3$, suggesting that $\epsilon^{2\alpha+1} = o(\epsilon^2)$, $\epsilon^3 = o(\epsilon^{2\alpha+1})$, $\epsilon^{2\beta+1} = o(\epsilon^2)$, and $\epsilon^3 = o(\epsilon^{2\beta+1})$. Then it can be checked straightforwardly that the balance equations at the first three orders are, respectively,

$$f_h^{(0)} = f_h^{(\text{eq})}, \tag{51a}$$

$$D_0 f_h^{(0)} = -\frac{1}{\tau} f_h^{(1)}, \tag{51b}$$

$$\partial_{t_1} f_h^{(0)} + D_0 f_h^{(1)} = -\frac{1}{\tau} f_h^{(2)}. \tag{51c}$$

However, the terms associated with Δx and Δt will affect the discrete balance equation at the order of ϵ^3, suggesting a consistent $f_h^{(3)}$ defined by Eq. (20) cannot be achieved. The proof is completed. ■

In summary, the arguments given in above subsections show that DUGKS is a consistent scheme for the kinetic Eq. (1) with uniform stability in ϵ, and with Theorem 1, it can be concluded that the DUGKS is a second-order UP scheme, which gives the Navier-Stokes solutions with numerical resolutions $\Delta t = o(\sqrt{\epsilon})$ and $\Delta x = o(\sqrt{\epsilon})$.

Remark 3. If the collision term is neglected in the reconstruction of the interface distribution function, i.e., $f_{j+1/2}^{n+1/2} = f_{j'}^n = (\frac{1}{2} - \beta) f_{j+1}^n + (\frac{1}{2} + \beta) f_j^n$, then the modified equation of this collision-less reconstruction (CLR) scheme is (see the Appendix for details)

$$\partial_t f_h + \xi \partial_x f_h + \frac{\Delta x^2}{6}\xi \partial_x^3 f_h + \frac{\Delta t}{2}\underbrace{\left[\partial_t^2 f_h - \xi^2 \partial_x^2 f_h - \frac{1}{\epsilon}\partial_t Q_h\right]}_{A'} = \frac{1}{\epsilon} Q_h + O(\Delta t^2)\mathcal{L}\left(\frac{1}{\epsilon} Q_h\right) + O(\Delta x^3, \Delta t \Delta x^2, \Delta t^2)\mathcal{L} f_h. \tag{52}$$

It can be shown that $A' = -\xi \partial_x \partial_t f_h - \xi^2 \partial_x^2 f_h + O(\Delta t, \Delta x^2)\mathcal{L} f_h$, and the modified equation can be rewritten as

$$\partial_t f_h + \xi \partial_x f_h + \frac{\Delta x^2}{6}\xi \partial_x^3 f_h - \frac{\Delta t}{2}\left(\xi \partial_x \partial_t f_h + \xi^2 \partial_x^2 f_h\right) = \frac{1}{\epsilon} Q_h + O(\Delta x^3, \Delta t^2), \tag{53}$$

which suggests that the UP order of the scheme would degenerate in comparison with the DUGKS due to the nonvanishing A' [see Eq. (43)]. As a result, under the same cell resolution the above scheme cannot give accurate Navier-Stokes solutions. This result confirms that it is important to consider the collision term in the reconstruction of numerical flux [29], and implies the essence of the temporal-spatial coupling in the design of schemes [28].

F. Numerical test

We now test the UP property of the DUGKS with the two-dimensional incompressible Taylor vortex in a periodic domain $0 \leqslant x \leqslant 1$ and $0 \leqslant y \leqslant 1$. At the hydrodynamic scale ($\epsilon \ll 1$), the flow is governed by the incompressible Navier-Stokes equations and has the following analytical solution,

$$u_x = -\frac{u_0}{A}\cos(Ax)\sin(By)e^{-\nu\theta t}, \tag{54a}$$

$$u_y = \frac{u_0}{B}\sin(Ax)\cos(By)e^{-\nu\theta t}, \tag{54b}$$

$$p(x, y, t) = p_0 - \frac{\rho_0 u_0^2}{4}\left[\frac{\cos(2Ax)}{A^2} + \frac{\cos(2By)}{B^2}\right]e^{-2\nu\alpha t}, \tag{54c}$$

where u_0 is a constant, $\theta = A^2 + B^2$, ν is the shear viscosity, and $\boldsymbol{u} = (u_x, u_y)$ and p are the velocity and pressure, respectively, $p_0 = \rho_0 R T_0$ is the reference pressure with ρ_0 the average density and T_0 the constant temperature.

For this low-speed isothermal flow, the discrete velocity set used in the DUGKS is chosen based on the three-point Gauss-Hermite quadrature in each direction as shown in Ref. [7], namely, $\boldsymbol{\xi}_0 = (0, 0)$, $\boldsymbol{\xi}_1 = -\boldsymbol{\xi}_3 = c(1, 0)$, $\boldsymbol{\xi}_2 = -\boldsymbol{\xi}_4 = c(0, 1)$, $\boldsymbol{\xi}_5 = -\boldsymbol{\xi}_7 = c(1, 1)$, $\boldsymbol{\xi}_6 = -\boldsymbol{\xi}_8 = c(-1, 1)$, with $c = \sqrt{3RT_0}$. The equilibrium distribution function is approximated

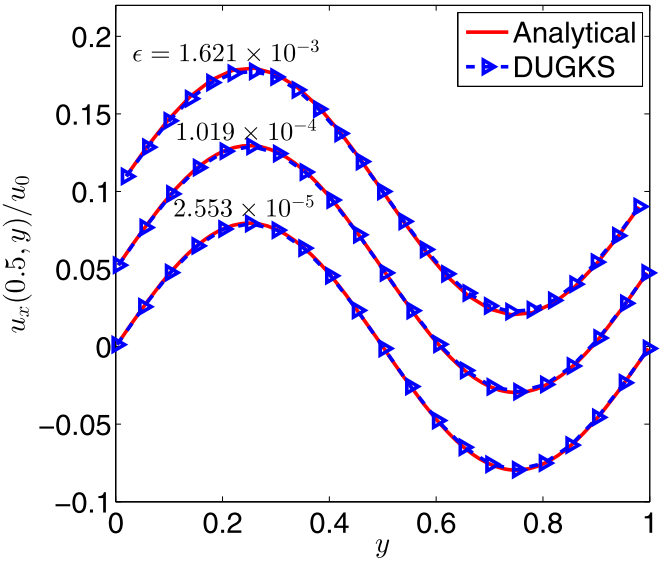

FIG. 3. Velocity profiles of the Taylor vortex flow at $t = t_c$ predicted by the DUGKS with $\Delta x = \sqrt{\epsilon}$. The profiles for $\epsilon = 1.621 \times 10^{-3}$ and 1.019×10^{-4} are shifted upward for clarity.

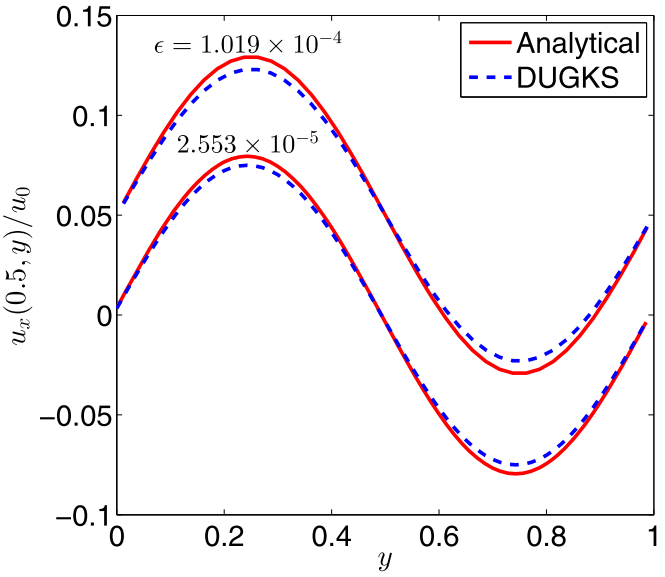

FIG. 4. Velocity profiles of the Taylor vortex flow at $t = t_c$ predicted by the DUGKS with $\Delta x \approx \epsilon^{0.4}$. The profile for 1.019×10^{-4} is shifted upward for clarity.

with the low Mach number expansion of the Maxwellian equilibrium,

$$f_i^{(\mathrm{eq})} = w_i \rho \left[1 + \frac{\boldsymbol{\xi}_i \cdot \boldsymbol{u}}{RT_0} + \frac{(\boldsymbol{\xi}_i \cdot \boldsymbol{u})^2}{2(RT_0)^2} - \frac{|\boldsymbol{u}|^2}{2RT_0} \right], \tag{55}$$

where $w_0 = 4/9$, $w_1 = w_2 = w_3 = w_4 = 1/9$, and $w_5 = w_6 = w_7 = w_8 = 1/36$. It is clear that these parameters are the same as the standard D2Q9 lattice Boltzmann equation model [2].

In our simulations, we set $A = B = 2\pi$, $u_0 = 0.01$, and $RT_0 = 0.5$, such that the Mach number is small and the flow can be well recognized as incompressible. The relaxation time is determined from the shear viscosity, $\tau = \nu/RT_0$ so that the parameter ϵ can be adjusted by changing the value of ν. Uniform meshes are employed and the CFL number η is set to be 0.5 for each mesh. Periodic boundary conditions are imposed on all boundaries, and the distribution functions are initialized by setting $f_i = f_i^{(eq)} + \epsilon f_i^{(1)}$, which is the Chapman-Enskog approximation at the Navier-Stokes order.

Three values of ϵ for continuum flow regime, i.e., 1.621×10^{-3}, 1.019×10^{-4}, and 2.553×10^{-5}, are considered in the simulations. We first test whether the Navier-Stokes solution for each case can be captured by the DUGKS with a uniform mesh with resolution of $\Delta x \sim \epsilon^{\alpha}$ with $\alpha = 0.501$, (and thus $\Delta t \sim \epsilon^{\alpha}$). Specifically, uniform meshes with size of 25×25, 100×100, and 200×200 are adopted for $\epsilon = 1.621 \times 10^{-3}$, 1.019×10^{-4}, and 2.553×10^{-5}, respectively. The velocity profiles at $t = t_c \equiv \ln 2/(\nu\theta)$, at which the magnitude of the velocity decays to one half of the original one, are measured and shown in Fig. 3. It can be observed that the velocity profiles are well captured by the DUGKS with the meshes, confirming its second-order UP property. We note that the mesh resolutions are much larger than the kinetic scale in the tests ($\Delta x/\epsilon = 24.68$, 98.18, and 195.81, respectively, for the three cases).

We then tests whether the DUGKS can capture the Navier-Stokes solutions with meshes of coarser resolution than $O(\epsilon^{0.5})$. As an example, we use a 40×40 mesh and a 70×70 one for $\epsilon = 1.019 \times 10^{-4}$ and 2.553×10^{-5}, respectively, such that $\Delta x \approx \epsilon^{0.4}$. The velocity profiles are shown in Fig. 4, and some clear deviations between the numerical and analytical solutions can be observed. These results confirm the UP analysis of DUGKS presented above, namely, Δx and Δt should be of $o(\epsilon^{0.5})$ to capture the Navier-Stokes hydrodynamics.

We now test whether the CLR scheme, where the distribution function $f_{j+1/2}^{n+1/2}$ is reconstructed by solving the collision-less kinetic equation as noted in Remark II and the Appendix, can capture the Navier-Stokes solutions with the same numerical resolution as used in the DUGKS (i.e., $\Delta x \sim \epsilon^{0.501}$ with CFL number $\eta = 0.5$). The predicated velocity profiles for $\epsilon = 1.621 \times 10^{-3}$, 1.019×10^{-4}, and 2.553×10^{-5} are shown in Fig. 5, which clearly demonstrates that the CLR scheme is too dissipative to capture the Navier-Stokes solutions under this cell resolution. These results confirm the UP property of this scheme shown in the Appendix.

V. EXAMPLE II: UP PROPERTIES OF A SECOND-ORDER IMEX RUNGE-KUTTA SCHEME

In this section we investigate the UP property of a second-order IMEX Runge-Kutta (IMEX-RK) scheme presented in Ref. [23]. Originally, the time asymptotics of the IMEX-RK scheme was analyzed in Ref. [23], in which the spatial gradient was considered to be exact. It was claimed that the scheme could capture the Navier-Stokes limit without resolving the kinetic scheme, i.e., as $\epsilon = o(\Delta t)$ and $\Delta t = o(\epsilon^{0.5})$. However, as we demonstrated in the introduction and Sec. IV, it is critical to consider the temporal-spatial coupling for the asymptotic behaviors of a multiscale kinetic scheme. We will

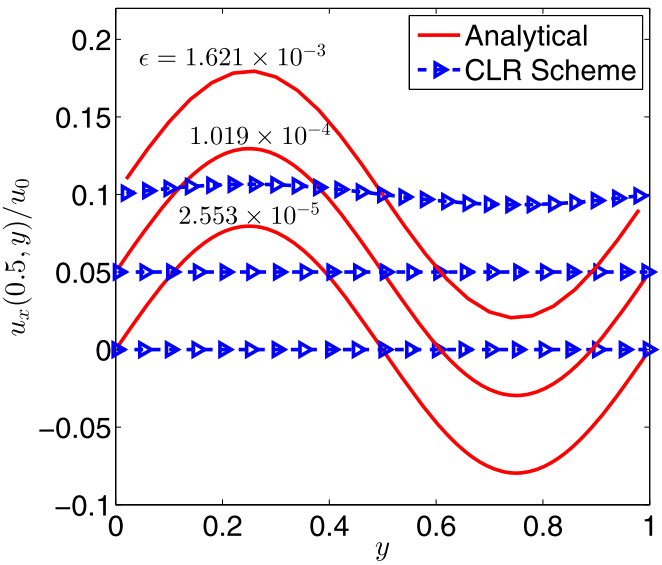

FIG. 5. Velocity profiles of the Taylor vortex flow at $t = t_c$ predicted by the CLR scheme with $\Delta x = \epsilon^{0.501}$. The profiles for $\epsilon = 1.621 \times 10^{-3}$ and 1.019×10^{-4} are shifted upward for clarity.

revisit this scheme in the UP framework to study how the spatial discretization influences the asymptotics.

A. Formulation

The second-order IMEX-RK scheme considered here is a two-stage globally stiffly accurate (GSA) one, which is named as IMEX-II-GSA(2,3,2) in Ref. [23]. In one dimension, the scheme can be expressed as

$$f_h^{n+1/2} = f_h^n - \frac{\xi\Delta t}{2}\partial_x f_h^n + \frac{\Delta t}{2\epsilon}Q_h^{n+1/2}, \tag{56a}$$

$$f_h^{n+1} = f_h^n - \Delta t\xi\partial_x f_h^{n+1/2} + \frac{\Delta t}{2\epsilon}\left[Q_h^n + Q_h^{n+1}\right], \tag{56b}$$

where the spatial derivatives are not discretized. Note that the hydrodynamic variables appearing in $f^{(\mathrm{eq})}$ of $Q^{n+1/2}$ and Q^{n+1} are first obtained from Eq. (56) by taking the conservative moments,

$$\bar{\mathbf{W}}_h^{n+1/2} = \bar{\mathbf{W}}_h^n - \frac{\Delta t}{2}\partial_x \boldsymbol{\mathcal{F}}_h^n, \tag{57a}$$

$$\bar{\mathbf{W}}_h^{n+1} = \bar{\mathbf{W}}_h^n - \frac{\Delta t}{2}\partial_x \boldsymbol{\mathcal{F}}_h^{n+1/2}, \tag{57b}$$

where $\bar{\mathbf{W}}_h = (\rho_h, \rho_h \boldsymbol{u}_h, \rho_h E_h)^T$ and $\boldsymbol{\mathcal{F}}_h = \int \boldsymbol{\xi}\boldsymbol{\psi} f_h d\boldsymbol{\xi}$.

B. Time asymptotics

From Eq. (56), we can obtain that

$$\frac{f_h^{n+1} - f_h^n}{\Delta t} + \xi\partial_x f_h^n - \frac{\Delta t}{2}\xi^2\partial_x^2 f_h^n + \frac{\Delta t}{2\epsilon}\partial_x Q_h^{n+1/2} = \frac{1}{2\epsilon}\left[Q_h^n + Q_h^{n+1}\right]. \tag{58}$$

By performing the Taylor expansions at t_n, we can obtain the modified equation of the IMEX-RK sheme,

$$\begin{aligned}\partial_t f_h + \xi\partial_x f_h + \frac{\Delta t}{2}\underbrace{\left[\partial_t^2 f_h - \xi^2\partial_x^2 f_h - \frac{1}{\epsilon}\partial_t Q_h + \frac{1}{\epsilon}\xi\partial_x Q_h\right]}_{A} \\ + \frac{\Delta t^2}{6}\underbrace{\left[\partial_t^3 f_h + \frac{3}{2\epsilon}\left(\xi\partial_x\partial_t Q_h - \partial_t^2 Q_h\right)\right]}_{B} + \frac{\Delta x^2}{6}\xi\partial_x^3 f_h \\ = \frac{1}{\epsilon}Q_h + O(\Delta t^3, \Delta t\Delta x^2)\mathcal{L}\left(\frac{1}{\epsilon}Q_h\right) \\ + O(\Delta x^3, \Delta t\Delta x^2, \Delta t^3)\mathcal{L}f_h,\end{aligned} \tag{59}$$

which is similar to the modified Eq. (40) for the DUGKS. Actually, the underbraced term A is the same as that in Eq. (40). Then, after some similar analysis we can obtain the simplified modeified equation for the IMEX-RK scheme,

$$\partial_t f_h + \xi\partial_x f_h + \frac{\Delta t^2}{6}B = \frac{1}{\epsilon}Q_h + O(\Delta x^3, \Delta t\Delta x^2, \Delta t^3)\mathcal{L}f_h, \tag{60}$$

with

$$B = -\tfrac{1}{2}\partial_t^3 f_h + \tfrac{3}{2}\xi^2\partial_x^2\partial_t f_h. \tag{61}$$

It is clear that the IMEX-RK is a second-order time discretization of the kinetic equation. Furthermore, it can be shown that if $\Delta t = O(\epsilon^\alpha)$ with $0.5 < \alpha < 1$, the IMEX-RK is second-order UP in time. This suggests that it can preserve the Navier-Stokes solution if $\Delta t = o(\epsilon^{0.5})$ and $\epsilon = o(\Delta t)$, which is consistent with the result in Ref. [23].

It should be noted, however, that the above analysis only considers the temporal discretization, and the spatial gradient is assumed to be exact. Since the kinetic equation is temporal-spatial coupled intrinsically, the temporal-spatial coupling at discrete level is also critical for a good practical numerical scheme [28]. This is also evident from the latter stability analysis and numerical results.

C. Uniform stability

The numerical stability of the IMEX-RK depends on the spatial discretization. If the space is discretized with a uniform mesh and the convection term is discretized with the second-order central difference scheme, then the IMEX-RK scheme (56) can be expressed as

$$f_j^{n+1/2} = f_j^n - \frac{\xi\Delta t}{2\Delta x}\left(f_{j+1/2}^n - f_{j+1/2}^n\right) + \frac{\Delta t}{2\epsilon}Q_j^{n+1/2}, \tag{62a}$$

$$f_j^{n+1} = f_j^n - \frac{\Delta t}{\Delta x}\left(f_{j+1/2}^{n+1/2} - f_{j+1/2}^{n+1/2}\right) + \frac{\Delta t}{2\epsilon}\left[Q_j^n + Q_j^{n+1}\right], \tag{62b}$$

where $f_j^n = f_h(x_j, t_n)$ and

$$f_{j+1/2}^n = \tfrac{1}{2}\left(f_j^n + f_{j+1}^n\right), \quad f_{j+1/2}^{n+1/2} = \tfrac{1}{2}\left(f_j^{n+1/2} + f_{j+1}^{n+1/2}\right), \tag{63}$$

which is similar with the linear reconstruction used in the DUGKS.

In the collisionless limit ($\epsilon \to \infty$), the IMEX-RK with the above spatial discretization becomes

$$\frac{f_j^{n+1} - f_j^n}{\Delta t} + \frac{\xi}{2\Delta x}\left(f_{j+1}^n - f_{j-1}^n\right) - \frac{\xi^2 \Delta t}{8\Delta x^2}\left(f_{j+2}^n - 2f_j^n + f_{j-2}^n\right) = 0, \tag{64}$$

which is similar with the case of the DUGKS, Eq. (37), except for the second term on the left hand side. Generally this term introduces artificial dissipation that can enhance numerical stability. However, it can be shown via the von Neumann analysis that the scheme (64) is *unconditionally unstable*. With a finite value of ϵ, the numerical stability of the IMEX-RK can be enhanced, but it is a nontrivial task to prove its stability property rigorously.

The above analysis indicates that the IMEX-RK with the second-order central difference discretization is not a legitimate scheme of the kinetic equation in the collisionless limit, and is not uniformly stable in terms of ϵ. Therefore, the IMEX-RK with such discretization is not a UP scheme. Particularly, this scheme cannot be applied to multiscale flows with a wide range of ϵ. Other types of spatial discretization methods can be employed to enhance the numerical stability. For example, a second-order finite-volume scheme with a slope limiter reconstruction was used in Ref. [19], and a fifth-order weighted essentially nonoscillatory (WENO) finite-difference method was employed in Ref. [23]. However, these methods may introduce additional numerical dissipation that destroys the UP property.

D. Numerical test

To test the capability of the IMEX-RK scheme in capturing the Navier-Stokes behavior, we now simulate the Taylor vortex problem with the same parameters as used in Sec. IV F. To overcome the numerical instability problem of the central difference discretization, an improved third-order WENO interpolation [43], with better numerical stability and accuracy than the classical WENO method, is employed to calculate $f_{j+1/2}$ in Eq. (62).

The velocity profiles at t_c for the three Knudsen numbers are shown in Fig. 6, with $\Delta x \approx \epsilon^{0.501}$. It can be seen that the numerical results predicted by the IMEX-RK scheme agree well with the analytical solutions for $\epsilon = 1.019 \times 10^{-4}$ and 2.553×10^{-5}, but deviation is clearly observed for the case of $\epsilon = 1.621 \times 10^{-3}$, which can be attributed to the relatively large numerical dissipation of the WENO interpolation near extremum points.

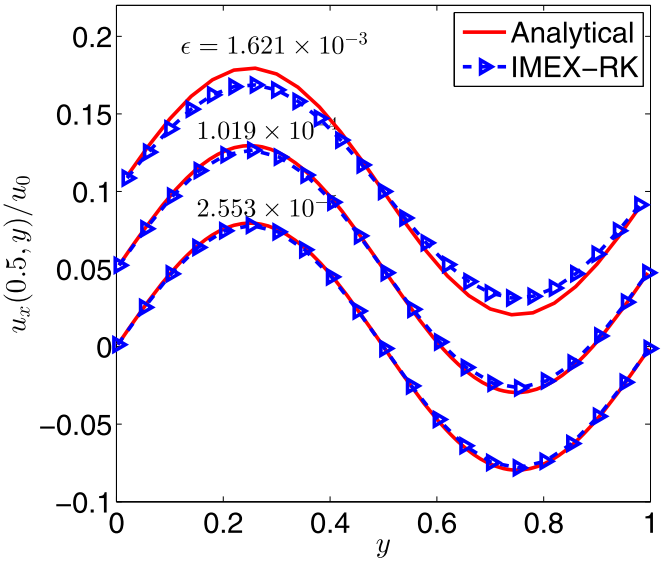

FIG. 6. Velocity profiles of the Taylor vortex flow at $t = t_c$ predicted by the IMEX-RK scheme with the improved third-order WENO interpolation and $\Delta x = \epsilon^{0.501}$. The profiles for $\epsilon = 1.621 \times 10^{-3}$ and 1.019×10^{-4} are shifted upward for clarity.

VI. SUMMARY AND DISCUSSIONS

For a kinetic scheme for multiscale flow simulations, it is required to capture the hydrodynamic behaviors in the continuum limit without resolving the kinetic scales, but with the cell resolution for distinguishing the hydrodynamic structure only. The asymptotic preserving (AP) concept is helpful for understanding the limiting behavior of a kinetic scheme as $\epsilon \to 0$, i.e., the dynamics described by the Euler equations. In the present work, we propose the unified preserving (UP) concept to distinguish the asymptotic behaviors of a kinetic scheme at small but nonzero ϵ and the order of asymptotics to capture the corresponding hydrodynamic structure.

We note that the role of the UP analysis is different from the general numerical analysis method for kinetic schemes aiming to solve certain hydrodynamic equations, such as the lattice Boltzmann equation and the gas-kinetic scheme. For such numerical methods, the target macroscopic (Euler or Navier-Stokes) equations to be solved are clearly specified, and the classical numerical analysis can provide useful information on how to choose the numerical parameters; however, the UP analysis is used mainly for kinetic schemes for simulating multiscale flows rather than for certain specific hydrodynamic equations. Actually, such a scheme can be viewed as a dynamic system on a finite mesh with discrete time, and its dynamic behavior depends on the numerical parameters (mesh size and time step) in addition to physical ones. Owing to the multiscale nature of the system, it is not clear what continuum hydrodynamic equations are solved by the kinetic scheme, or even no well-posed hydrodynamics models are available. The goal of the UP analysis is just to identify the hydrodynamic behaviors under different numerical parameters.

Generally, a UP scheme with order $n \geqslant 1$ is also AP, and therefore the UP concept can be viewed as an extension of the AP concept. But it should be noted that the approach for analyzing the UP properties is different from that for analyzing the AP property of a kinetic scheme. In the AP analysis, the corresponding discrete formulation of the kinetic scheme as $\epsilon \to 0$ is first derived, and then is proved to be a consistent and stable discretization of the corresponding hydrodynamic equations. However, in the UP framework the analysis is based on the Chapman-Enskog expansion of the modified equation of the kinetic scheme, and the expansion coefficients at different orders of ϵ can be compared with those of the original Chapman-Enskog expansion of the ki-

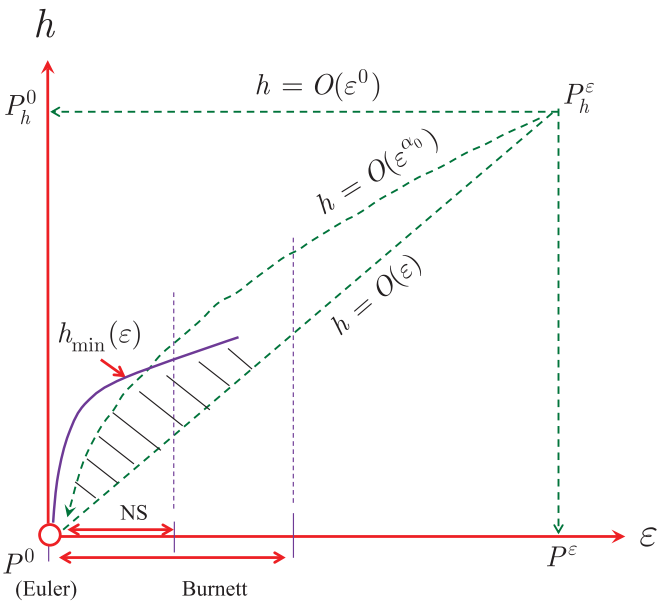

FIG. 7. Schematic of asymptotic path to the limiting hydrodynamic regimes with flow structures. The lines are similar with those shown in Fig. 2, and the line $h_{\min}(\epsilon)$ represents the minimum resolution required by flow structures. The shadowed region represents the parameter space for a UP scheme.

netic equation and thus the asymptotic degree of accuracy can be assessed.

The UP order of a kinetic scheme depends on three scales, i.e., kinetic scale $(\hat{\lambda}_0, \hat{\tau}_0)$, numerical scale $(\Delta\hat{x}, \Delta\hat{t})$, and hydrodynamic scale $(\hat{l}_0, \hat{t}_0)$. Specifically, the order is related to the dimensionless parameters $\epsilon = \hat{\tau}_0/\hat{t}_0 = \hat{\lambda}_0/\hat{l}_0$, $\delta_x = \Delta\hat{x}/\hat{\lambda}_0$, and $\delta_t = \Delta\hat{t}/\hat{\tau}_0$. Furthermore, the accuracies of spatial and temporal discretizations also affect the UP order. In general, for given cell size and time step scalings, the UP order increases with the accuracy order of the scheme. It is emphasized here that the present work assumes the numerical resolution is adequate to resolve the flow physics at the hydrodynamic limit. For practical problems with flow structures (such as boundary layer, shear layer, shock layer, and oscillation period) some restrictions to the mesh size and/or time step are required. For instance, to capture the shock structure, whose thickness is of $O(\epsilon)$ [44], a mesh size of $O(\epsilon)$ is necessary. Under such circumstance, the numerical resolution h should be not larger than an ϵ-dependent minimum $h_{\min}(\epsilon)$, which is an additional imposition on the UP scheme. Consequently, the parameter space of the kinetic scheme to approach its asymptotic limit may be changed, as demonstrated in Fig. 7. Only as the numerical resolution of the scheme falls in the shadowed region, the kinetic scheme can capture the correct hydrodynamic behaviors without resolving the kinetic scale. The main target for the UP analysis is to evaluate the kinetic schemes whether they can recover the shock capturing schemes for the NS solutions in the hydrodynamic flow regime, such as the laminar boundary layer, without imposing kinetic scale resolution on the mesh size and time step.

As an example, the UP property of a temporal-spatial discretized kinetic scheme, DUGKS, is first analyzed. It is shown that the DUGKS is a second-order UP scheme which can capture hydrodynamics at the Navier-Stokes level without resolving the kinetic scale, and the numerical test confirms the property. However, if the distribution function at cell interface is reconstructed by solving the collision-less kinetic equation, then the scheme is only of first-order UP under the same numerical resolution. The results confirm the necessity of the inclusion of collision effect in the reconstruction. We note that some kinetic schemes also consider the collision effect in flux reconstruction [6,45], and it would be interesting to analyze the UP properties of these schemes. The UP property of a second-order time-discrete scheme, IMEX-RK, is further analyzed. It is shown the scheme is of second-order time UP provided the spatial gradient is exact. However, if the second-order central-difference (i.e., linear reconstruction) is used as in the DUGKS, the IMEX-RK is not uniformly stable, and thus is not UP. The use of a third-order improved WENO interpolation can enhance the numerical stability, but numerical results demonstrate that the numerical dissipation arising from spatial discretization can destroy the UP property. These findings again confirm the necessity of considering the fully temporal-spatial particle transport and collision coupling in designing a UP kinetic scheme.

The UP property discussed in this study is focused on the case of hydrodynamic regime where ϵ is small, which is the key requirement for kinetic schemes. For flows beyond the continuum regime, the solution of a UP scheme is expected to be able to capture the noncontinuum flow physics since the scheme is consistent with the kinetic equation. For instance, the DUGKS has been successfully applied to a variety of nonequilibrium flows ranging from slip to free-molecular regimes [30].

Finally, we remark that other techniques rather than the original Chapman-Enskog expansion can also be employed to analyze the asymptotic property of a kinetic scheme in the UP framework, such as the regularized Chapman-Enskog expansions [36–38], the Maxwell iteration procedure [46], or the order-of-magnitude method [47,48].

ACKNOWLEDGMENTS

Z.L.G. acknowledges the support by the National Natural Science Foundation of China (Grants No. 51836003 and No. 11872024). J.Q.L. was supported by National Natural Science Foundation of China (Grants No. 11771054, No. 12072042, and No. 91852207) and the Sino-German Research Group Project (Grant No. GZ1465). K.X. was supported by Hong Kong Research Grant Council (Grant No. 16208021) and National Natural Science Foundation of China (Grants No. 11772281 and No. 91852114). Helpful discussions with Dr. S. Chen and Dr. C. Liu are gratefully acknowledged.

APPENDIX: UP ANALYSIS OF THE CLR SCHEME

In this Appendix we will derive the modified equation of the CLR kinetic scheme noted in Remark 3 in which the cell-interface distribution function $f_{j+1/2}^{n+1/2}$ is reconstructed from the collision-less BGK equation,

$$f_{j+1/2}^{n+1/2} = f_{j'}^{n} = \left(\tfrac{1}{2} - \beta\right) f_{j+1}^{n} + \left(\tfrac{1}{2} + \beta\right) f_{j}^{n}. \tag{A1}$$

Then we have

$$\frac{f_{j+1/2}^{n+1/2}-f_{j-1/2}^{n+1/2}}{\Delta x}=\partial_x f_h+\frac{\Delta x^2}{6}\partial_x^3 f_h-\frac{\Delta t}{2}\xi\partial_x^2 f_h + O(\Delta x^3,\Delta t\Delta x^2)\mathcal{L}f_h. \tag{A2}$$

The modified equation can thus be derived as

$$\partial_t f_h+\xi\partial_x f_h+\frac{\Delta t}{2}\underbrace{\left[\partial_t^2 f_h-\xi^2\partial_x^2 f_h-\frac{1}{\epsilon}\partial_t Q_h\right]}_{A'}+\frac{\Delta x^2}{6}\xi\partial_x^3 f_h = \frac{1}{\epsilon}Q_h+O(\Delta t^2)\mathcal{L}\left(\frac{1}{\epsilon}Q_h\right)+O(\Delta x^3,\Delta t\Delta x^2,\Delta t^2)\mathcal{L}f_h. \tag{A3}$$

With this equation we can estimate the underbraced term A',

$$\begin{aligned}A'&=(\partial_t-\xi\partial_x)\left(\partial_t f_h+\xi\partial_x f_h-\frac{1}{\epsilon}Q_h\right)-\frac{1}{\epsilon}\xi\partial_x Q_h\\&=\frac{\Delta t}{2}(\xi\partial_x-\partial_t)A'-\frac{1}{\epsilon}\xi\partial_x Q_h+O(\Delta t^2)\mathcal{L}\left(\frac{1}{\epsilon}Q_h\right)\\&\quad+O(\Delta x^2,\Delta t^2)\mathcal{L}f_h,\end{aligned} \tag{A4}$$

which leads to

$$A'=-\frac{1}{\epsilon}\xi\partial_x Q_h+O(\Delta t)\mathcal{L}\left(\frac{1}{\epsilon}Q_h\right)+O(\Delta x^2,\Delta t^2)\mathcal{L}f_h. \tag{A5}$$

Therefore, the modified Eq. (A3) can be rewritten as

$$\partial_t f_h+\xi\partial_x f_h-\frac{\Delta t}{2\epsilon}\xi\partial_x Q_h+\frac{\Delta x^2}{6}\xi\partial_x^3 f_h = \frac{1}{\epsilon}Q_h+O(\Delta t^2)\mathcal{L}\left(\frac{1}{\epsilon}Q_h\right)+O(\Delta x^3,\Delta t\Delta x^2,\Delta t^3)\mathcal{L}f_h, \tag{A6}$$

from which we can obtain that

$$\frac{1}{\epsilon}Q_h=\partial_t f_h+\xi\partial_x f_h+O(\Delta t,\Delta x^2)\mathcal{L}f_h. \tag{A7}$$

Thus,

$$\begin{aligned}A'&=-\frac{1}{\epsilon}\xi\partial_x Q_h+O(\Delta t,\Delta x^2)\mathcal{L}f_h\\&=-\xi\partial_x\partial_t f_h-\xi^2\partial_x^2 f_h+O(\Delta t,\Delta x^2)\mathcal{L}f_h,\end{aligned} \tag{A8}$$

and the modified Eq. (A6) can be re-expressed as

$$\partial_t f_h+\xi\partial_x f_h-\frac{\Delta t}{2}\left(\xi\partial_x\partial_t f_h+\xi^2\partial_x^2 f_h\right)+\frac{\Delta x^2}{6}\xi\partial_x^3 f_h = \frac{1}{\epsilon}Q_h+O(\Delta x^3,\Delta t^2), \tag{A9}$$

which shows that the time accuracy of this CLR scheme is of first order.

As $\Delta t=O(\epsilon^\alpha)$ and $\Delta x=O(\epsilon^\beta)$ with $0.5<\alpha,\beta<1$, Eq. (A9) can be reformulated as (with only error terms of leading order),

$$\epsilon\partial_t f_h+\epsilon\xi\partial_x f_h-\epsilon^{1+\alpha}\frac{a}{2}\left(\xi\partial_x\partial_t f_h+\xi^2\partial_x^2 f_h\right)+\epsilon^{2\beta+1}\frac{b}{6}\xi\partial_x^3 f_h = -\frac{1}{\tau}\left(f_h-f_h^{(\mathrm{eq})}\right), \tag{A10}$$

where $a=O(1)$ and $b=O(1)$. From Eq. (A10) we can obtain the first two Chapman-Enskog expansion coefficients of f_h

$$\epsilon^0:\quad f_h^{(0)}=f_h^{(\mathrm{eq})}, \tag{A11a}$$

$$\epsilon^1:\quad D_0 f_h^{(0)}=-\frac{1}{\tau}f_h^{(1)}. \tag{A11b}$$

However, the coefficient $f_h^{(2)}$ cannot be determined due to the appearing of term of $O(\epsilon^{1+\alpha})$. This suggests that CLR scheme is of first-order UP and the Navier-Stokes solution cannot be captured by this scheme under the same numerical resolution as the DUGKS, i.e., $\Delta t=O(\epsilon^\alpha)$ and $\Delta x=O(\epsilon^\beta)$ with $0.5<\alpha,\beta<1$.

It is interesting that as $\Delta t=o(\epsilon)$ and $\Delta x=o(\epsilon^{1/2})$, namely, $\Delta t=O(\epsilon^\alpha)$ and $\Delta x=O(\epsilon^\beta)$ with $\alpha>1$ and $\beta>0.5$, we can obtain the balance equation for $f_h^{(2)}$ exactly. However, this means that the time step Δt must resolve the kinetic time scale to capture the Navier-Stokes solutions, which indicates that the CLR scheme is not an UP solver and is inapplicable to multiscale flows. The above analysis confirms the fact that it is necessary to consider the collision effect in the reconstruction of the cell-interface distribution function in developing UP kinetic schemes.

[1] K. Xu and C. Liu, Phys. Fluids **29**, 026101 (2017).

[2] Z. L. Guo and C. Shu, *Lattice Boltzmann Method and Its Applications in Engineering* (World Scientific, Singapore, 2013).

[3] K. Xu, J. Comput. Phys. **171**, 289 (2001).

[4] P. Santagati, G. Russo, and S. B. Yun, SIAM J. Numer. Anal. **50**, 1111 (2012).

[5] G. Dimarco and L. Pareschi, SIAM J. Numer. Anal. **51**, 1064 (2013). **55**, 664 (2017); S. Pieraccini and G. Puppo, J. Sci. Comput. **32**, 1 (2007); J. W. Hu, R. W. Shu, and X. X. Zhang, SIAM J. Numer. Anal. **56**, 942 (2018).

[6] K. Xu and J. C. Huang, J. Comput. Phys. **229**, 7747 (2010).

[7] Z. L. Guo, R. J. Wang, and K. Xu, Phys. Rev. E **91**, 033313 (2015); Z. L. Guo, K. Xu, and R. J. Wang, *ibid.* **88**, 033305 (2013); Z. L. Guo and K. Xu, Adv. Aerodyn. **3**, 6 (2021).

[8] G. Dimarco and L. Pareschi, Acta Numerica **23**, 369 (2014).

[9] S. Jin, SIAM J. Sci. Comput. **21**, 441 (1999); Riv. Mat. Univ. Parma **3**, 177 (2012).

[10] J. W. Hu, S. Jin, and Q. Li, in *Handbook of Numerical Methods for Hyperbolic Problems* (North-Holland, Amsterdam, 2017), pp. 103–129.

[11] E. W. Larsen, Nucl. Sci. Eng. **83**, 90 (1983).

[12] E. W. Larsen, J. Morel, and J. Miller, J. Comput. Phys. **69**, 283 (1987).

[13] A. Klar, SIAM J. Numer. Anal. **35**, 1073 (1998).
[14] S. Jin, J. Comput. Phys. **122**, 51 (1995); L. Pareschi and G. Russo, in *Hyperbolic Problems: Theory, Numerics, Applications* (Springer, Berlin, 2003), pp. 241–251.
[15] R. B. Lowrie and J. E. Morel, Int. J. Numer. Meth. Fluids **40**, 413 (2002).
[16] F. Coron and B. Perthame, SIAM J. Numer. Anal. **28**, 26 (1991).
[17] A. Klar, SIAM J. Numer. Anal. **36**, 1507 (1999).
[18] M. Bennoune, M. Lemou, and L. Mieussens, J. Comput. Phys. **227**, 3781 (2008).
[19] F. Filbet and S. Jin, J. Comput. Phys. **229**, 7625 (2010).
[20] L. Mieussens, AIP Conf. Proc. **1628**, 943 (2014).
[21] F. G. Tcheremissine, in *Hyperbolic Problems: Theory, Numerics, Applications* (Springer, Berlin, 2001), pp. 883–890.
[22] A. Klar, J. Comput. Phys. **148**, 416 (1999).
[23] J. W. Hu and X. X. Zhang, J. Sci. Comput. **73**, 797 (2017).
[24] T. Xiong, J. Jang, F. Y. Li, and J.-M. Qiu, J. Comput. Phys. **284**, 70 (2015).
[25] M. Seaïd and A. Klar, Comput. Fluids **35**, 872 (2006).
[26] S. Boscarino and L. Pareschi, J. Comput. Appl. Math. **316**, 60 (2017).
[27] S. Jin and C. D. Levermore, J. Comput. Phys. **126**, 449 (1996).
[28] J. Q. Li, Adv. Aerodyn. **1**, 3 (2019); J. Q. Li and Z. F. Du, SIAM J. Sci. Comput. **38**, A3046 (2016); L. Pan, K. Xu, Q. B. Li, and J. Q. Li, J. Comput. Phys. **326**, 197 (2016).
[29] S. Z. Chen and K. Xu, J. Comput. Phys. **288**, 52 (2015).
[30] P. Wang, M. T. Ho, L. Wu, Z. L. Guo, and Y. H. Zhang, Comput. Fluids **161**, 33 (2018); L. H. Zhu, S. Z. Chen, and Z. L. Guo, Comput. Phys. Commun. **213**, 155 (2017); L. Zhu and Z. Guo, Phys. Rev. E **95**, 023113 (2017); L. H. Zhu, X. F. Yang, and Z. L. Guo, Phys. Rev. Fluids **2**, 123402 (2017).
[31] R. F. Warming and B. J. Hyett, J. Comput. Phys. **14**, 159 (1974).
[32] J. Q. Li and Z. C. Yang, Appl. Math. Comput. **225**, 610 (2013).
[33] S. Chapman and T. Cowling, *The Mathematical Theory of Nonuniform Gases* (Cambridge University Press, Cambridge, UK, 1970).
[34] C. Cercignani, *The Boltzmann Equation and its Applications* (Springer-Verlag, New York, NY, 1988).
[35] A. N. Gorban and I. V. Karlin, Bull. Amer. Math. Soc. **51**, 187 (2014).
[36] P. Rosenau, Phys. Rev. A **40**, 7193 (1989).
[37] M. Slemrod, Physica D **109**, 257 (1997).
[38] A. N. Gorban and I. V. Karlin, Transp. Theor. Stat. Phys. **21**, 101 (1992).
[39] M. Slemrod, Quart. Appl. Math. **70**, 613 (2012).
[40] A. J. Wagner, Phys. Rev. E **74**, 056703 (2006); R. Z. Huang and H. Y. Wu, J. Comput. Phys. **327**, 121 (2016); L. Zheng, Q. L. Zhai, and S. Zheng, Phys. Rev. E **95**, 043301 (2017).
[41] K. Xu and Z. H. Li, J. Fluid Mech. **513**, 87 (2004).
[42] M. Junk and W.-A. Yong, Asymptotic Anal. **35**, 165 (2003); M. Junk, A. Klar, and L.-S. Luo, J. Comput. Phys. **210**, 676 (2005).
[43] N. K. Yamaleev and M. H. Carpenter, J. Comput. Phys. **228**, 3025 (2013).
[44] G. A. Bird and J. M. Brady, *Molecular Gas Dynamics and the Direct Simulation of Gas Flows*, Vol. 42 (Clarendon Press, Oxford, UK, 1994).
[45] D. W. Jiang, M. L. Mao, J. Li, and X. G. Deng, Adv. Aerodyn. **1**, 8 (2019).
[46] S. Harris, *An Introduction to the Theory of the Boltzmann Equation* (Dover Publications, Oxford, UK, 2011).
[47] H. Struchtrup, Phys. Fluids **16**, 3921 (2004).
[48] P. Kauf, M. Torrilhon, and M. Junk, J. Stat. Phys. **141**, 848 (2010).